© 2019. Published by The Company of Biologists Ltd | Journal of Cell Science (2019) 132, jcs232645. doi:10.1242/jcs.232645

RESEARCH ARTICLE

VLA-4 phosphorylation during tumor and immune cell migration relies on its coupling to VEGFR2 and CXCR4 by syndecan-1

Oisun Jung[1,2], DeannaLee M. Beauvais[1], Kristin M. Adams[1] and Alan C. Rapraeger[1,2,*]

ABSTRACT

When targeted by the tumor-promoting enzyme heparanase, cleaved and shed syndecan-1 (Sdc1) then couples VEGFR2 (also known as KDR) to VLA-4, activating VEGFR2 and the directed migration of myeloma cells. But how VEGFR2 activates VLA-4-mediated motility has remained unknown. We now report that VEGFR2 causes PKA-mediated phosphorylation of VLA-4 on S988, an event known to stimulate tumor metastasis while suppressing cytotoxic immune cells. A key partner in this mechanism is the chemokine receptor CXCR4, a well-known mediator of cell motility in response to gradients of the chemokine SDF-1 (also known as CXCL12). The entire machinery necessary to phosphorylate VLA-4, consisting of CXCR4, AC7 (also known as ADCY7) and PKA, is constitutively associated with VEGFR2 and is localized to the integrin by Sdc1. VEGFR2 carries out the novel phosphorylation of Y135 within the DRY microswitch of CXCR4, sequentially activating $G\alpha_i\beta\gamma$, AC7 and PKA, which phosphorylates S988 on the integrin. This mechanism is blocked by a syndecan-mimetic peptide ($SSTN_{VEGFR2}$), which, by preventing VEGFR2 linkage to VLA-4, arrests tumor cell migration that depends on VLA-4 phosphorylation and stimulates the LFA-1-mediated migration of cytotoxic leukocytes.

KEY WORDS: CXCR4, VEGFR2, KDR, Immune surveillance, Metastasis, Syndecan, Synstatin

INTRODUCTION

Very late antigen-4 (VLA-4, α4β1 integrin) has key roles in angiogenesis, immunity and tumor metastasis (Schlesinger and Bendas, 2015). It mediates endothelial cell migration during angiogenesis and lymphangiogenesis (Garmy-Susini et al., 2010; Jin et al., 2006) and induces the extravasation of tumor cells and tumor-promoting immunosuppressor cells including tumor-associated macrophages (TAMs), regulatory T cells (T_{regs}), and myeloid-derived suppressor cells (MDSCs) from the vasculature to sites of tumor formation (Alon et al., 1995; Ding et al., 2001; Juneja et al., 1993; Schlesinger and Bendas, 2015; Taichman et al., 1991). VLA-4 recognizes fibronectin (FN) within the stromal matrix and also interacts with vascular cell adhesion molecule-1 (VCAM-1) on endothelial and stromal cells (Hemler et al., 1990). It is regulated via an intricate signaling mechanism in which VLA-4 localized at the cell's leading edge undergoes cAMP-dependent protein kinase (PKA)-mediated phosphorylation of serine 988 (S988) in the α4 integrin cytoplasmic domain. This displaces paxillin and its associated Arf GAP from the integrin, thereby facilitating localized RAC1 activation, lamellipodium formation and directional cell migration (Goldfinger et al., 2003; Nishiya et al., 2005). In contrast, VLA-4 phosphorylation suppresses the influx of tumor-inhibiting natural killer (NK) and cytotoxic thymus-derived (T) cells, because displacement of paxillin from VLA-4 also displaces PYK2 and FAK kinases needed for transregulation of lymphocyte function-associated antigen 1 (LFA-1, αLβ2 integrin) that these cells need for their migration (Cantor et al., 2015; Feral et al., 2006). However, despite these essential roles for VLA-4 phosphorylation during immune surveillance and cancer invasion, the key events controlling VLA-4 phosphorylation remain unknown.

The C-X-C chemokine receptor 4 (CXCR4) is a member of the G protein-coupled receptor superfamily of proteins, comprising over 800 members (Fredriksson et al., 2003). It plays a key role in many physiological and pathological processes including progenitor cell migration during development, neovascularization, immunity and inflammatory diseases (Balkwill, 2004). It is upregulated in numerous human cancers, where it stimulates metastasis in response to gradients of stromal cell-derived factor-1 (SDF-1, also known as C-X-C chemokine ligand 12, CXCL12) (Balkwill, 2004; Teicher and Fricker, 2010; Walenkamp et al., 2017). Like VLA-4, CXCR4 is also thought to support tumor growth by promoting invasion of immunosuppressive cells while impairing the influx of cytotoxic cells to tumor sites (Fearon, 2016; Han et al., 2015).

Vascular endothelial growth factor receptor-2 (VEGFR2, also known as KDR) is a type II transmembrane tyrosine kinase receptor mainly expressed on endothelial cells, and is a key mediator of endothelial tip cell migration during sprouting angiogenesis (Blanco and Gerhardt, 2013). However, it is also expressed by many cancer cells (Goel and Mercurio, 2013) and correlates with increased tumor metastasis (Jach et al., 2010; Jung et al., 2016; Kopparapu et al., 2013). Moreover, it also contributes to immunosuppression during tumor progression (Gavalas et al., 2012; Goel and Mercurio, 2013; Horikawa et al., 2017; Kaur et al., 2014; Tada et al., 2018; Zhu et al., 2017; Ziogas et al., 2012).

We now report a novel finding in which these three key regulators, CXCR4, VLA-4 and VEGFR2, are united in a common mechanism by the cell surface proteoglycan syndecan-1 (Sdc1) to regulate directed cell migration across a spectrum of cell types. We have shown previously in myeloma and vascular endothelial cells that a docking site in the Sdc1 extracellular domain, active only when cleaved from its transmembrane domain by matrix metallopeptidase 9 (MMP9), couples VEGFR2 to VLA-4 clustered at the cell's leading edge (Jung et al., 2016). This coupling activates VEGFR2, which, via an unknown mechanism, activates VLA-4-mediated invasion (Jung et al., 2016). In this current work, we now demonstrate that VEGFR2 acts as a scaffold for the entire machinery

[1]Department of Human Oncology, School of Medicine and Public Health, University of Wisconsin-Madison, 1111 Highland Avenue, Madison, WI 53705, USA. [2]Graduate Program in Molecular and Cellular Pharmacology, School of Medicine and Public Health, University of Wisconsin-Madison, 1111 Highland Avenue, Madison, WI 53705, USA.

*Author for correspondence (rapraeger@humonc.wisc.edu)

O.J., 0000-0002-4099-6274; A.C.R., 0000-0003-1719-3286

Received 8 April 2019; Accepted 20 September 2019

Journal of Cell Science (2019) 132, jcs232645. doi:10.1242/jcs.232645

necessary for phosphorylation of VLA-4 on S988. The machinery consists of CXCR4 and its $G\alpha_i\beta\gamma$ heterotrimeric G-protein, a Gβγ-dependent adenylate cyclase (AC7, also known as ADCY7) and PKA that targets S988 on the integrin. The activation mechanism acts only when VEGFR2 is coupled to the integrin by shed Sdc1, which can be prevented by an inhibitory peptide mimetic of the Sdc1 docking site ('synstatin-VEGFR2' or '$SSTN_{VEGFR2}$'). A key feature is activation of CXCR4, which occurs either in response to SDF-1, or when the VEGFR2 kinase phosphorylates tyrosine 135 (Y135) within the CXCR4 aspartate–arginine–tyrosine (DRY) regulatory motif (Fredriksson et al., 2003).

RESULTS

Shed Sdc1-mediated VEGFR2 activation causes phosphorylation of the α4 integrin subunit on S988

Heparanase (HPSE)-mediated trimming of the heparan sulfate (HS) chains on Sdc1 induces shedding of its extracellular domain (sSdc1), allowing sSdc1 to assemble into a ternary complex with VEGFR2 and VLA-4. This causes VEGFR2 activation by transphosphorylation, triggering polarized cell migration (Jung et al., 2016). Migration is blocked by (i) HPSE or MMP9 inhibitors that prevent Sdc1 shedding, (ii) a peptide ($SSTN_{VEGFR2}$) that competes for the Sdc1 binding site on VEGFR2, or (iii) by expressing Sdc1 lacking a functional VEGFR2 docking site ($Sdc1^{\Delta PVD}$) (Jung et al., 2016). To test whether activation of VEGFR2 when docked with Sdc1 causes phosphorylation of S988 in the cytoplasmic domain of the α4 integrin subunit of VLA-4, endogenous human Sdc1 (hSdc1) expression was silenced in CAG^{HPSE} myeloma cells (a myeloma cell line expressing high levels of HPSE), HMEC-1 microvascular endothelial cells, or M14 melanoma cells. Silencing hSdc1 largely abolishes α4-S988 phosphorylation, which is fully rescued by expression of mouse Sdc1 (mSdc1), but not by $mSdc1^{\Delta PVD}$, which fails to engage VEGFR2 (Fig. 1A). Furthermore, treatment with HPSE inhibitor (OGT2115), $SSTN_{VEGFR2}$, VEGFR2 kinase inhibitor (vandetanib), or PKA kinase inhibitor (H-89) all abolish integrin phosphorylation, implicating each of these targets in a common regulatory mechanism (Fig. 1B). The importance of α4-pS988 in cell migration is confirmed by silencing α4 integrin expression, which completely blocks transfilter migration towards IIICS, a recombinant fragment of FN containing the VLA-4 binding region (Massia and Hubbell, 1992), and rescue of migration by transient re-expression of wild-type (WT) α4 integrin subunit but not by a phosphorylation-resistant S988A mutant (Goldfinger et al., 2003) (Fig. 1C,D). Transfilter migration is also blocked by $SSTN_{VEGFR2}$, vandetanib or H-89 (Fig. 1C,E), which is reversed by transient expression of a phosphomimetic α4-S988D mutant (Fig. 1C,E), indicating that integrin phosphorylation is the ultimate target of the Sdc1-mediated mechanism.

VEGFR2 activates and links PKA to VLA-4

PKA is known to phosphorylate S988 in the α4 integrin subunit (Goldfinger et al., 2008). Testing whether PKA activation depends on sSdc1, we find that phosphorylation of T197 in PKA's activation loop is reduced by $SSTN_{VEGFR2}$ (Fig. 2A). Furthermore, inhibition of VEGFR2 kinase by vandetanib dramatically reduces VLA-4-dependent migration, which is fully restored by 6-Bnz-cAMP, a selective PKA activator (Fig. 2B; Fig. S1). In line with this observation, vandetanib and H-89 (PKA inhibitor) also reduce PKA and α4 integrin phosphorylation, mimicking $SSTN_{VEGFR2}$ (Fig. 2C). 6-Bnz-cAMP rescues PKA and α4 integrin phosphorylation in the presence of vandetanib (Fig. 2C), consistent with its rescue of cell migration (Fig. 2B). However, despite activating PKA, it fails to rescue either α4 integrin phosphorylation or cell migration when VEGFR2 coupling to VLA-4 by sSdc1 is prevented by $SSTN_{VEGFR2}$ (Fig. 2B,C; Fig. S1). This is explained by our finding that PKA associates with both VEGFR2 and VLA-4 when the proteins are precipitated individually, consistent with their assembly into a single complex by sSdc1, but PKA precipitates only with VEGFR2 when VLA-4 is displaced by $SSTN_{VEGFR2}$ (Fig. 2D), suggesting that PKA is localized to its target (VLA-4) by its association with VEGFR2.

AC7 is required for PKA activation

Activation of PKA within the receptor complex suggests the involvement of an adenylate cyclase (AC) and upstream heterotrimeric G-protein. The latter has been identified as a $G\alpha_i$-containing G-protein by treatment with pertussis toxin (PTX) (Hofer and Lefkimmiatis, 2007; Katada, 2012), which blocks cell migration that is fully rescued by 6-Bnz-cAMP (Fig. 3A). This is further confirmed by the reduction in cellular levels of active $G\alpha_i$ ($GTP\text{-}G\alpha_i$) observed after PTX, vandetanib or $SSTN_{VEGFR2}$ treatment (Fig. 3B). ADP ribosylation of the $G\alpha_i$ subunit by PTX prevents interaction between the G protein and G protein-coupled receptor (GPCR), blocking nucleotide exchange and activation of $G\alpha_i$. PTX also prevents the release of active Gβγ (Smrcka, 2008) and stimulation of AC isoforms activated by free Gβγ, namely AC2, AC4 (also known as ADCY2 and ADCY4) and AC7 (Sunahara and Taussig, 2002). We find that Gβγ is involved because gallein, a specific Gβγ inhibitor, blocks PKA T197 phosphorylation (Fig. 3C) and inhibits VLA-4-dependent migration by all three cell types, which is rescued by 6-Bnz-cAMP or forskolin, an adenylate cyclase activator (Fig. 3D; Fig. S2B). Furthermore, silencing Gβγ-dependent AC7, but not AC2 or AC4, expression blocks VLA-4-dependent migration (Fig. 3E,F; Fig. S2C), which is rescued by 6-Bnz-cAMP (Fig. 3G; Fig. S2D), and dramatically reduces PKA-mediated α4 integrin phosphorylation (Fig. 3F). These results delineate a $G\alpha_i\beta\gamma \rightarrow AC7 \rightarrow cAMP \rightarrow PKA$ signaling pathway that activates VLA-4-dependent migration of myeloma, melanoma and endothelial cells.

CXCR4 activates VLA-4-dependent cell migration in a ligand-independent manner

The Sdc1-coupled mechanism appears to depend on CXCR4, a $G\alpha_i$-coupled receptor previously implicated in VLA-4 and/or VEGFR2 function (Guerin et al., 2008; Ngo et al., 2008; Sanz-Rodriguez et al., 2001), because silencing CXCR4 expression with siRNAs abolishes VLA-4-dependent migration by myeloma, endothelial and melanoma cells (Fig. 4A; Fig. S3A) and reduces PKA T197 and α4 integrin S988 phosphorylation (Fig. 4B). In contrast, silencing expression of CXCR3, another abundant chemokine receptor expressed by these cells, does not affect their VLA-4 mediated cell migration (Fig. S3B–D). To test whether CXCR4 depends on SDF-1, the VLA-4-adherent cells were stimulated with SDF-1 or, conversely, were treated with either SDF-1-blocking antibody or AMD3100, an antagonist of SDF-1 binding to CXCR4. SDF-1 enhances cell migration by 25–50% in all three cell types (Fig. 4C; Fig. S3E). Whereas CXCR4-blocking antibody and AMD3100 have no effect on unstimulated cell migration, both significantly reduce SDF-1-stimulated migration to levels witnessed in the absence of SDF-1 (Fig. 4C; Fig. S3E). SDF-1 rescues migration of vandetanib-treated cells (Fig. 4D; Fig. S3F), suggesting the existence of a VEGFR2 kinase-dependent CXCR4 activation mechanism in addition to the SDF-1-dependent mechanism. However, SDF-1-mediated activation also depends on VEGFR2, as it cannot rescue the block to migration observed

Journal of Cell Science (2019) 132, jcs232645. doi:10.1242/jcs.232645

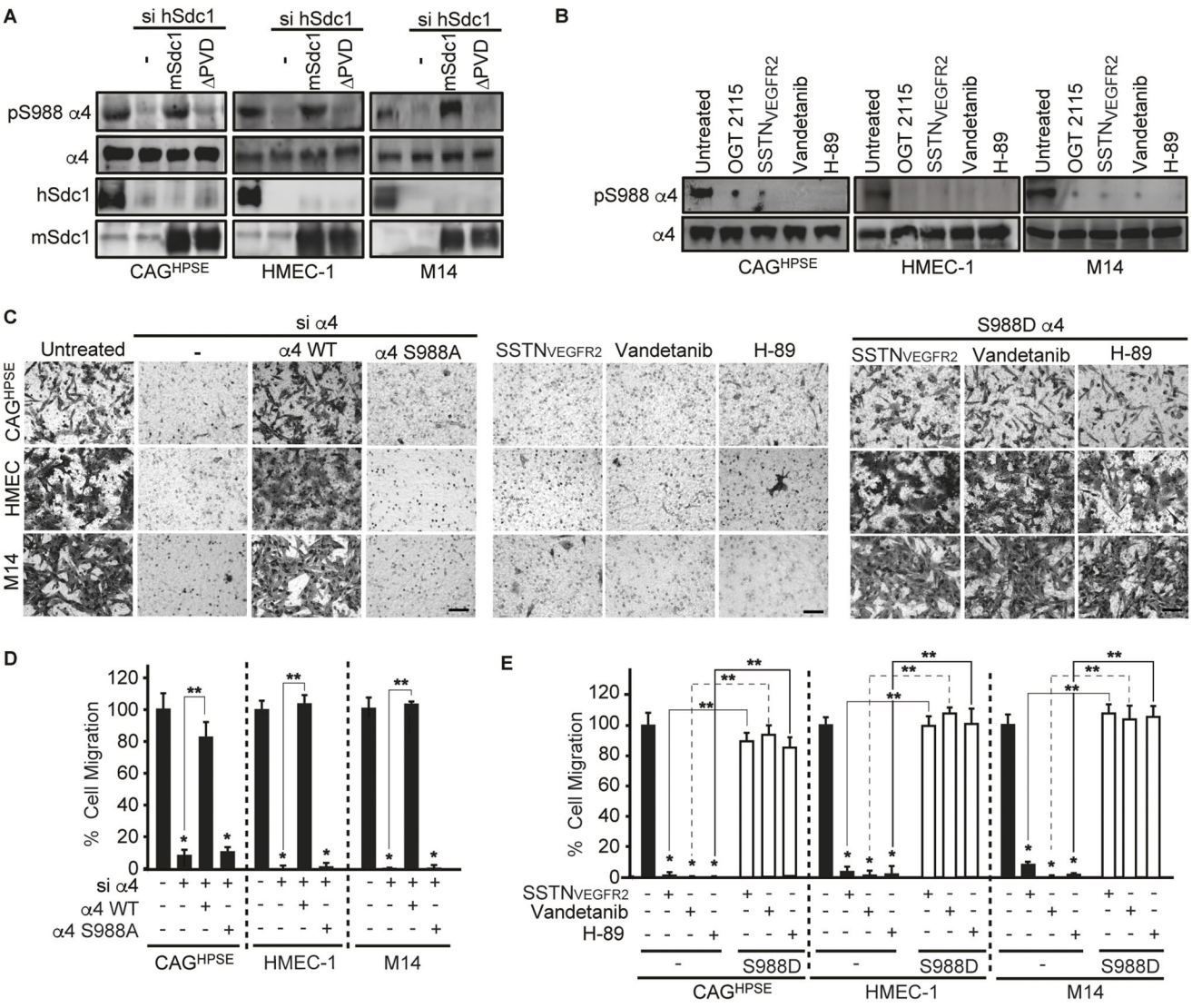

Fig. 1. VLA-4 phosphorylation at S988 is dependent on shed Sdc1-mediated VEGFR2 activation. (A) CAG^{HPSE}, HMEC-1 or M14 cells were co-transfected with or without small interfering RNA (si) against human (h)Sdc1 and cDNA constructs for mouse (m)Sdc1 or mSdc1$^{\Delta PVD}$. After 72 h, the cells were plated on 100 µg/ml IIICS for 2.5 h and lysates were analyzed by immunoblotting with an anti-α4-pS988, anti-total α4 integrin, anti-hSdc1 or anti-mSdc1 antibodies. (B) Cells were plated on 100 µg/ml IIICS in the absence or presence of 10 µM OGT2115 (HPSE inhibitor), 30 µM SSTN$_{VEGFR2}$, 10 µM vandetanib (VEGFR2 inhibitor), or 10 µM H-89 (PKA inhibitor). The whole-cell lysates were analyzed by immunoblotting with anti-α4-pS988 and anti-total α4 integrin antibody. (C–E) CAG^{HPSE}, HMEC-1 or M14 cells were co-transfected with or without siRNA against α4 integrin and siRNA-resistant cDNA constructs for HA-tagged WT, S988A or S988D α4 integrin for 48 h. Cells were allowed to migrate towards 100 µg/ml IIICS in the absence or presence of 30 µM SSTN$_{VEGFR2}$, 10 µM vandetanib, or 10 µM H-89 for 16 h. (C) Cells accumulated on the bottom side of the filter were imaged at 20× magnification. Scale bars: 50 µm. (D,E) Migrated cells were quantified from five random images for each condition and graphed as the mean±s.d. from three independent experiments. All data were compared using the unpaired one-tailed *t*-test. **P*<0.01 against untreated parental cells; ***P*<0.01 between treatments.

when VEGFR2 expression is silenced or if the coupling of VEGFR2 to VLA-4 is blocked by SSTN$_{VEGFR2}$ (Fig. 4D; Fig. S3F). This suggests that the entire machinery necessary to carry out VLA-4 phosphorylation on S988 either in response to adhesion or SDF-1 stimulation may be pre-assembled with VEGFR2. Indeed, CXCR4, AC7, PKA, Sdc1 and α4 integrin all co-immunoprecipitate with VEGFR2 (Fig. 4E). Furthermore, CXCR4, AC7 and PKA continue to co-immunoprecipitate with VEGFR2 when displaced from Sdc1 and VLA-4 by SSTN$_{VEGFR2}$ (Fig. 4E). Alternatively, silencing Sdc1, which prevents VEGFR2 interaction with VLA-4, does not affect its interaction with CXCR4, AC7 and PKA (Fig. 4F). In contrast, silencing VEGFR2 expression disrupts the co-precipitation of CXCR4, AC7 and PKA with Sdc1, whereas VLA-4 (as detected by the α4 integrin subunit) still precipitates with the syndecan (Fig. 4G). Further, silencing CXCR4 expression reduces Gβγ and AC7 precipitation with VEGFR2, but PKA remains associated (Fig. 4H), suggesting that PKA and CXCR4 associate independently with VEGFR2, whereas AC7 likely associates with CXCR4. As a specificity control, we examined the effects of SSTN$_{VEGFR2}$ on another Sdc1-organized receptor complex expressed on these cells, namely IGF1R and the αvβ3 or αvβ5 integrins captured by amino acids 93–120 in the extracellular domain of Sdc1 (Beauvais et al., 2016; Beauvais and Rapraeger, 2010). SSTN$_{VEGFR2}$ does not disrupt this complex, as shown by the continued co-precipitation of Sdc1 and αv integrin subunit with IGF1R in the presence of the peptide (Fig. S3G), nor

Journal of Cell Science (2019) 132, jcs232645. doi:10.1242/jcs.232645

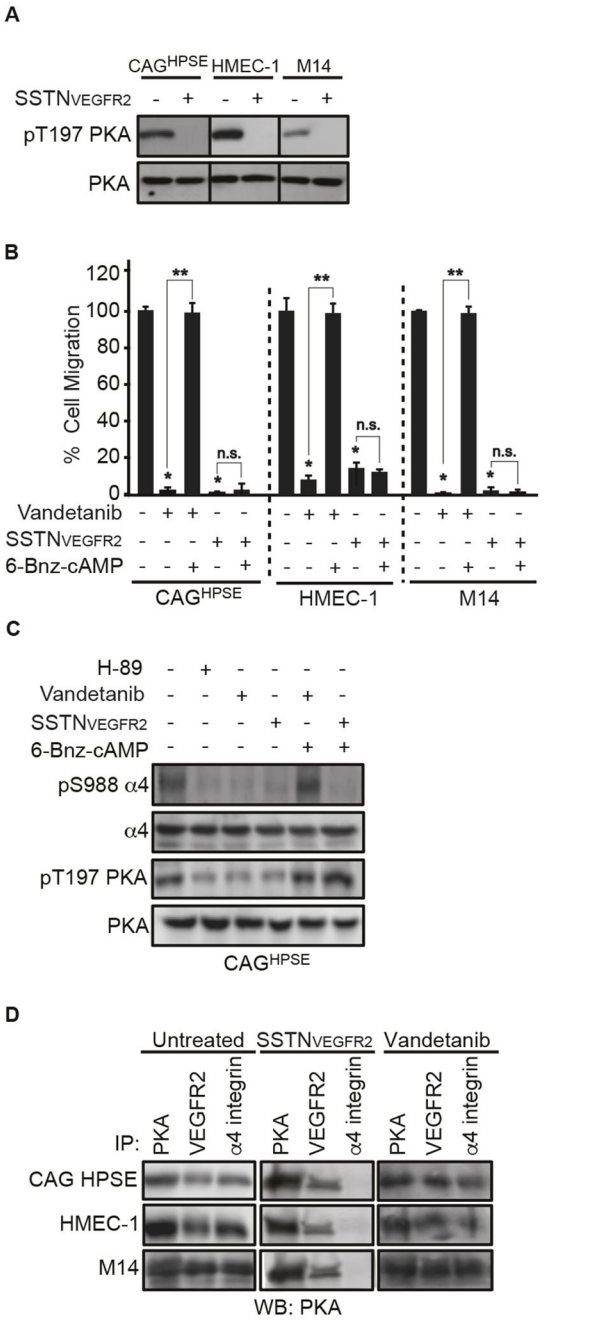

Fig. 2. Sdc1 activates PKA by coupling VEGFR2 to VLA-4. (A) CAG^{HPSE}, HMEC-1 or M14 cells were plated on 100 µg/ml IIICS with or without 30 µM SSTN$_{VEGFR2}$ for 2 h. Lysates were examined by immunoblotting with anti-pT197 PKA and anti-total PKA antibody. (B) 16 h transfilter migration assays towards 100 µg/ml IIICS were performed with CAG^{HPSE}, HMEC-1 or M14 cells in the absence or presence of 10 µM vandetanib, or 30 µM SSTN$_{VEGFR2}$ with or without 100 µM 6-Bnz-cAMP. Migrated cells were quantified in five random images for each condition and graphed as the mean±s.d. from three independent experiments. All data were compared using the unpaired one-tailed *t*-test. **P*<0.01 against untreated parental cells; ***P*<0.01, n.s., not significant between treatments. (C) CAG^{HPSE} cells were plated on 100 µg/ml IIICS in the absence or presence of 10 µM H-89, 10 µM vandetanib, or 30 µM SSTN$_{VEGFR2}$ with or without 100 µM 6-Bnz-cAMP. Whole-cell lysates were examined by immunoblotting with anti-α4 integrin (pS988 and total) and anti-PKA (pT197 and total) antibodies. (D) CAG^{HPSE}, HMEC-1 or M14 cells were plated on 100 µg/ml IIICS in the absence or presence of 30 µM SSTN$_{VEGFR2}$ or 10 µM vandetanib for 2 h, then whole-cell lysates were subjected to immunoprecipitation with an anti-PKA, anti-VEGFR2 or anti-α4 integrin antibody. Precipitated complexes were examined by immunoblotting for PKA.

does SSTN$_{IGF1R}$, a specific competitor of Sdc1–IGF1R–αvβ3/αvβ5 integrin assembly, prevent co-precipitation of CXCR4, AC7, PKA, VLA-4 and Sdc1 with VEGFR2 (Fig. S3G). Note that the Sdc1 blot is probed with antibodies directed either at the Sdc1 extracellular domain (ecto Sdc1) or its cytoplasmic domain (cyto Sdc1), the latter to detect only intact Sdc1 and demonstrate that only the shed form participates in VEGFR2 binding.

VEGFR2 activates CXCR4 by phosphorylating Y135 in its regulatory DRY motif

CXCR4 has six cytoplasmic tyrosine residues. One of these, tyrosine 135 (Y135), is localized to the highly conserved aspartate–arginine–tyrosine (DRY) activation motif found in the intracellular loop 2 of class A G-protein coupled receptors (GPCRs), including CXCR4 (Rovati et al., 2007). Although controversial, it is generally suggested that the DRY motif forms a lock, established by ionic or nonionic interactions with residues in transmembrane domain 6 that constrain receptor activation. Arginine 134 (R134) within this motif appears to have the additional role of engaging Gα_i and maintaining its inactive state. SDF-1 binding to the receptor's external N-terminus and extracellular loop 2 activates the G-protein by altering the tilt of transmembrane domain 3, which abolishes these interactions and activates the G-protein (Audet and Bouvier, 2012; Rovati et al., 2007; Salon et al., 2011; Wescott et al., 2016; Wu et al., 2010). Our discovery that VEGFR2 can activate CXCR4 independently of SDF-1 suggests that the kinase accomplishes the same outcome as SDF-1 binding, possibly by phosphorylating a critical tyrosine in one of the CXCR4 cytoplasmic loops, most likely Y135 itself within the DRY motif. This hypothesis is supported by the detection of tyrosine-phosphorylated CXCR4 immunoprecipitated from whole-cell lysates, which is abolished after vandetanib or SSTN$_{VEGFR2}$ treatment (Fig. 5A). To test which of the six cytoplasmic tyrosines might be targeted, we made single Y65F, Y76F, Y135F, Y157F, Y219F and Y302F point mutants that were ectopically expressed as GFP-fusion proteins in cells co-transfected with siRNA to silence their endogenous CXCR4 (Fig. 5B–F). Each of the mutants were expressed equally at the cell surface as native proteins as assessed by flow cytometric analysis of SDF-1 binding (Fig. 5B; Fig. S4), and all associate with each component of the sSdc1-organized complex indistinguishably from wild-type (WT) CXCR4 (Fig. 5C). Each mutant was also able to rescue VEGFR2-dependent CXCR4 tyrosine phosphorylation, except for the Y135F mutant (Fig. 5D), which also failed to rescue VLA-4-dependent cell migration when endogenous CXCR4 expression is silenced (Fig. 5E; Fig. S5). Nonetheless, the Y135F mutant did rescue migration if activated by SDF-1, confirming that it remains functional despite its failure to be activated by VEGFR2 (Fig. 5E; Fig. S5).

Next, we find that each of the CXCR4 tyrosine mutants – except for the Y135F mutant – generate GTP-loaded Gα_i and cause its dissociation from CXCR4 in response to VLA-4-mediated adhesion (Fig. 5F). Furthermore, Gα_i is activated in response to SDF-1 by all of the mutants, including Y135F, even in the presence of vandetanib (Fig. 5F). Lastly, a phosphomimetic CXCR4 mutant (Y135D) fully rescues cell migration when endogenous CXCR4 is silenced, but unlike wild-type CXCR4, the Y135D mutant is also able to rescue cell migration in response to VLA-4 engagement despite the presence of the VEGFR2 inhibitor vandetanib in all three cell types (Fig. 6A; Fig. S6). Consistent with these results, expression of the Y135D mutant also rescues GTP-loaded Gα_i levels and α4 integrin phosphorylation in the presence of the VEGFR2 kinase inhibitors vandetanib and VEGFR2 II (Fig. 6B), suggesting that Y135 in the DRY motif is likely to be the target of VEGFR2-mediated CXCR4

Journal of Cell Science (2019) 132, jcs232645. doi:10.1242/jcs.232645

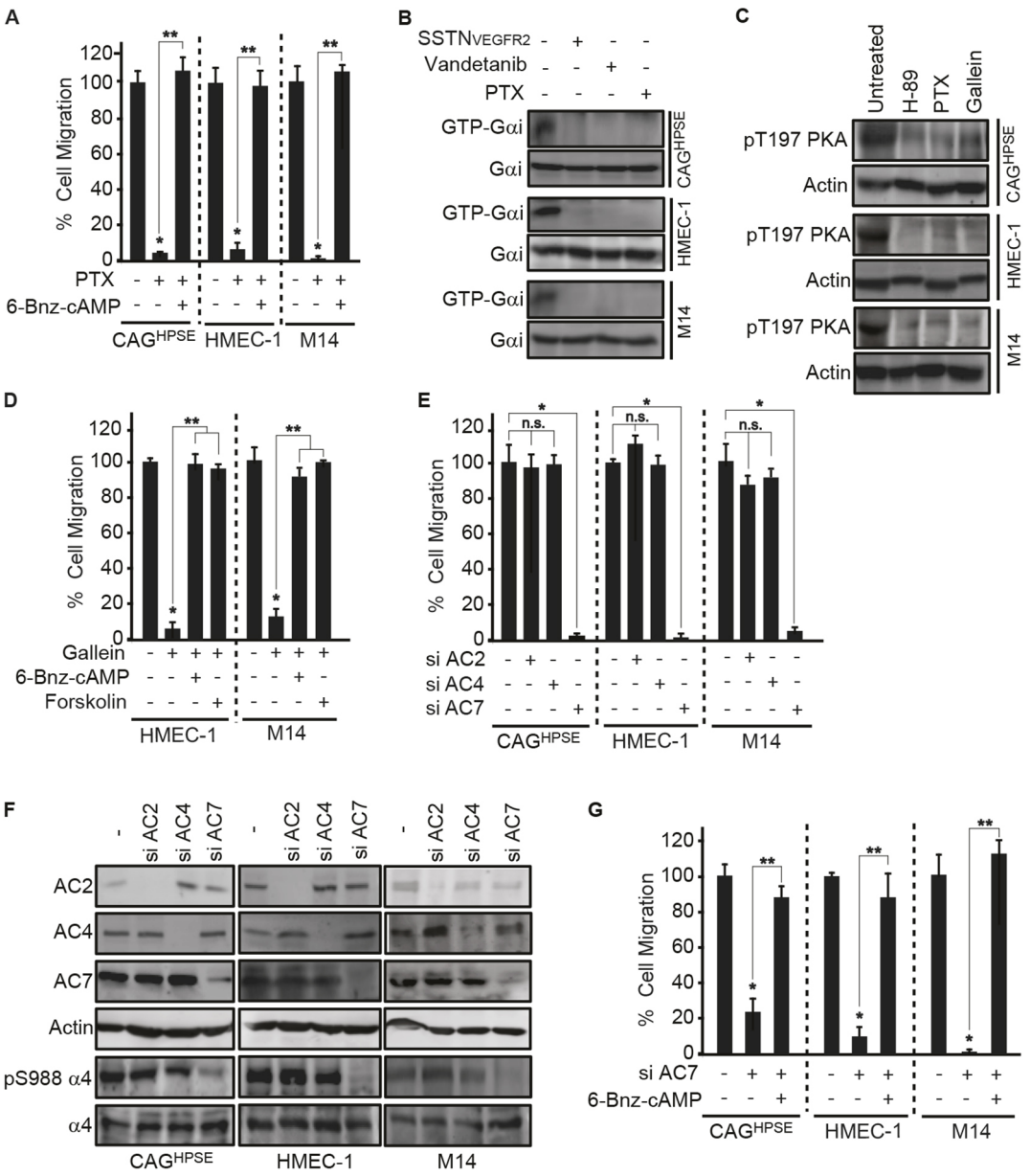

Fig. 3. Gβγ-dependent adenylate cyclase 7 activation is required for PKA activation. (A) 16 h transfilter migration assays towards 100 µg/ml IIICS were performed with CAG^{HPSE}, HMEC-1 or M14 cells in the absence or presence of 10 µg/ml pertussis toxin (PTX), with or without 100 µM 6-Bnz-cAMP. Migrated cells were quantified and graphed as the mean±s.d. from three independent experiments. All data were compared using the unpaired one-tailed *t*-test. **P*<0.01 against untreated parental cells; ***P*<0.01 between treatments. (B) CAG^{HPSE}, HMEC-1 or M14 cells were plated on 100 µg/ml IIICS with 30 µM SSTN$_{VEGFR2}$, 10 µg/ml vandetanib or 10 µg/ml PTX for 2 h. Whole-cell lysates were subjected to immunoprecipitation with an anti-GTP-Gα$_i$ antibody and immunoblotting for Gα$_i$. (C) CAG^{HPSE}, HMEC-1 or M14 cells were plated on 100 µg/ml IIICS with 10 µM H-89, 10 µg/ml PTX or 20 µM gallein for 2 h. Lysates were analyzed by immunoblotting for PKA pT197 or β-actin as a loading control. (D) 16 h transfilter migration assays towards 100 µg/ml IIICS were performed with HMEC-1 or M14 cells in the absence or presence of 20 µM gallein with or without 100 µM 6-Bnz-cAMP or 30 µM forskolin. Migrated cells were quantified and graphed as the mean±s.d. from three independent experiments. All data were compared using the unpaired one-tailed *t*-test. **P*<0.01 against untreated parental cells; ***P*<0.01 between treatments. (E,F) CAG^{HPSE}, HMEC-1 or M14 cells were transfected with siRNA against AC2, AC4 or AC7 for 48 h, before performing migration and immunoblotting assays. (E) 16 h transfilter migration assays towards 100 µg/ml IIICS were performed with CAG^{HPSE}, HMEC-1 or M14 cells. Migrated cells were quantified and graphed as the mean±s.d. from three independent experiments. All data were compared using the unpaired one-tailed *t*-test. **P*<0.01 against untreated parental cells; n.s., not significant between treatments. (F) Cell lysates were analyzed by immunoblotting for AC2, AC4, AC7, α4 integrin, α4-pS988 and β-actin as a loading control. (G) CAG^{HPSE}, HMEC-1 or M14 cells were transfected with or without AC7 siRNA for 48 h and then 16 h transfilter cell migration assays towards 100 µg/ml IIICS were performed in the absence or presence of 100 µM 6-Bnz-cAMP. Migrated cells were quantified and graphed as the mean±s.d. from three independent experiments. All data were compared using the unpaired one-tailed *t*-test. **P*<0.01 against untreated parental cells; ***P*<0.01 between treatments.

tyrosine phosphorylation, providing an alternate means of activation of CXCR4 and its heterotrimeric G-protein in the absence of ligand binding.

Taken together, these findings outline a molecular mechanism through which VEGFR2 (pre-associated with CXCR4, PKA and the PKA activation machinery), coupled to VLA-4 by shed Sdc1,

Journal of Cell Science (2019) 132, jcs232645. doi:10.1242/jcs.232645

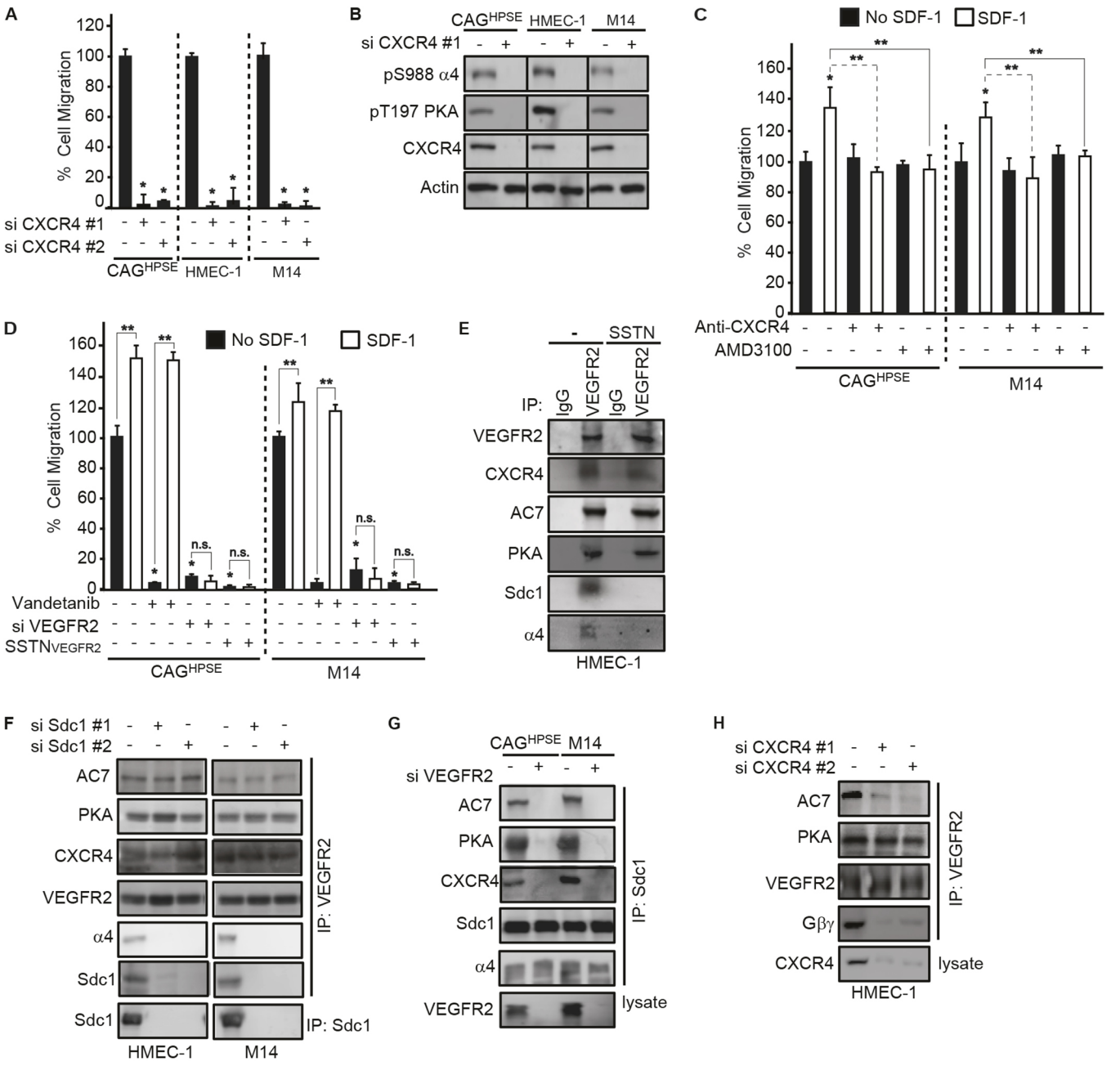

Fig. 4. See next page for legend.

leads to phosphorylation of S988 in VLA-4 and is blocked by $SSTN_{VEGFR2}$ (see model, Fig. 6C).

Coupling of VEGFR2 to VLA-4 by shed Sdc1 suppresses LFA-1-mediated migration of T cells and NK cells

When appropriately stimulated, cytotoxic NK and T lymphocytes rapidly extravasate across the vascular endothelium, relying on engagement with the endothelial cell-surface receptors ICAM-1 (a ligand for LFA-1) and VCAM-1 (a ligand for VLA-4). VLA-4 adhesion to VCAM-1 recruits paxillin and its associated FAK and PYK2 kinases to the integrin that activates LFA-1 via 'transregulation', leading to their ICAM-1-dependent diapedesis across the endothelium (see model in Fig. 7G). The Ginsberg group has elegantly shown that this is prevented by phosphorylation of integrin α4-S988 (Rose et al., 2003) and demonstrated the significance of this transregulation during tumor surveillance using genetically engineered ITGA4-S988A mutant mice (Cantor et al., 2015). When VLA-4 phosphorylation is prevented, this greatly enhances LFA-1-dependent influx of tumor-suppressing cytotoxic T lymphocytes and reduces growth of melanoma tumors. This suggests a possible role for the Sdc1-mediated mechanism (see Fig. 6C) not only in promoting the migration of tumor and endothelial cells, but also as an inhibitor of tumor immune surveillance. We therefore isolated primary mouse T cells and NK cells to test whether their migration is suppressed by VLA-4 phosphorylation, and whether $SSTN_{VEGFR2}$ might promote their migration through a mixture of ICAM-1 and VCAM-1 that mimics the endothelium during inflammation or cancer. We find that all the elements of the Sdc1 mechanism are expressed by NK cells and T cells (Fig. 7A), including VLA-4 phosphorylated on S988

Fig. 4. CXCR4 is required for VLA-4-dependent cell migration in a ligand-independent manner. (A) CAG^{HPSE}, HMEC-1 or M14 cells were transfected with two different CXCR4 siRNAs for 48 h prior to 16 h transfilter migration assays towards 100 µg/ml IIICS. Migrated cells were quantified and graphed as the mean±s.d. from three independent experiments. All data were compared using the unpaired one-tailed *t*-test. **P*<0.01 against untreated parental cells. (B) CAG^{HPSE}, HMEC-1 or M14 cells transfected with CXCR4 siRNA for 48 h were analyzed by immunoblotting for integrin α4-pS988, PKA pT197, CXCR4 or β-actin. (C) 16 h transfilter migration assays towards IIICS were performed with CAG^{HPSE} and M14 cells treated with or without 10 µg/ml CXCR4-blocking antibody or 10 µM AMD3100 in the absence or presence of 20 ng/ml SDF-1. Migrated cells were quantified and graphed as the mean±s.d. from three independent experiments. All data were compared using the unpaired one-tailed *t*-test. **P*<0.01 against untreated parental cells; ***P*<0.01 between treatments. (D) CAG^{HPSE} or M14 cells were transfected with or without VEGFR2 siRNA for 48 h. 16 h transfilter migration assays towards 100 µg/ml IIICS were performed with or without 30 µM SSTN$_{VEGFR2}$ or 10 µM vandetanib. Migrated cells were quantified and graphed as the mean±s.d. from three independent experiments. All data were compared using the unpaired one-tailed *t*-test. **P*<0.01 against untreated parental cells; ***P*<0.01, n.s., not significant between treatments. (E) HMEC-1 cells were plated on 100 µg/ml IIICS with 30 µM SSTN$_{VEGFR2}$ for 2.5 h. Cell lysates were subjected to immunoprecipitation with rabbit anti-VEGFR2 antibody. The VEGFR2-associated complexes were analyzed by immunoblotting for VEGFR2 (with mouse anti-VEGFR2), CXCR4, AC7, PKA, hSdc1 or α4 integrin. (F) HMEC-1 or M14 cells were transfected with two different Sdc1 siRNA for 48 h and plated on 100 µg/ml IIICS for 2 h. Cell lysates were subjected to immunoprecipitation with rabbit anti-VEGFR2. The associated complexes were probed with mouse anti-VEGFR2, anti-CXCR4, anti-α4 integrin, anti-AC7, anti-hSdc1 or anti-PKA antibodies. Silencing of Sdc1 expression was confirmed by immunoprecipitation with rabbit polyclonal anti-Sdc1 and probed with mouse anti-human Sdc1 antibody. (G) CAG^{HPSE} or M14 cells were transfected with VEGFR2 siRNAs for 48 h and plated on 100 µg/ml IIICS for 2 h. Cell lysates were subjected to immunoprecipitation with rabbit polyclonal anti-Sdc1 antibody. The associated complexes were analyzed by immunoblotting for AC7, PKA, CXCR4, Sdc1 or α4 integrin. The whole-cell lysates were analyzed by immunoblotting for VEGFR2. (H) HMEC-1 cells were transfected with two different CXCR4 siRNAs for 48 h and then cell lysates were subjected to immunoprecipitation with anti-VEGFR2 antibody. The associated complexes were analyzed by immunoblotting for AC7, PKA, VEGFR2 or Gβγ. The whole-cell lysates were analyzed by immunoblotting for CXCR4.

(Fig. 7B) and that Sdc1, VLA-4, CXCR4, AC7 and PKA co-immunoprecipitate with VEGFR2 when these cells are plated on VCAM-1, but are displaced by SSTN$_{VEGFR2}$ (Fig. 7B). No association is observed between VEGFR2 and VLA-5 ($\alpha_5\beta_1$ integrin) or LFA-1 ($\alpha_L\beta_2$ integrin) used as controls (Fig. 7B). Furthermore, pS988-VLA-4 co-localizes with VEGFR2 and Sdc1 at the surface of T cells and NK cells plated on VCAM-1 (Fig. S7A).

Testing the relative importance of VLA-4 and LFA-1 in these cells, we confirm that their adhesion to VCAM-1 is blocked by VLA-4-inhibitory antibodies (Fig. 7C). However, the cells fail to migrate on this substratum under any conditions tested (Fig. 7D,E). The cells adhere to ICAM-1 via LFA-1 (Fig. 7C) and their attachment is blocked by LFA-1-inhibitory antibodies, but this requires treatment with SDF-1, consistent with previously published reports (Peled et al., 2000; Wu et al., 2012). Although the mechanism of LFA-1 activation by SDF-1 is unknown, it does not appear to involve its binding to CXCR4 as AMD3100 fails to inhibit attachment (Fig. 7C; Fig. S7B). Despite the ability of the cells to adhere to ICAM-1, they fail to migrate through transfilters coated with ICAM-1 alone or a mixture of ICAM-1 and VCAM-1 (Fig. 7D; Fig. S7C). However, this is reversed by SSTN$_{VEGFR2}$ treatment (Fig. 7D; Fig. S7C), suggesting that the Sdc1-coupled phosphorylation machinery (see Fig. 7G) constitutively suppresses their ability to migrate. Whereas SSTN$_{VEGFR2}$-stimulated NK cells migrate on ICAM-1 alone, T cells require co-stimulation with VCAM-1 (Fig. 7D), consistent with prior reports that NK cells express a population of constitutively active VLA-4 that transregulates LFA-1, whereas T cells require VCAM-1 to activate VLA-4 and its transregulation of LFA-1 (Rose et al., 2000, 2001). VCAM-1 also enhances the SSTN$_{VEGFR2}$-stimulated NK cell migration on ICAM-1, which is reduced down to the constitutive levels of LFA-1-dependent migration by VLA-4-blocking antibody (Fig. 7D). In order to mimic SSTN$_{VEGFR2}$-induced cell migration on mixed ICAM-1–VCAM-1 substrata, we blocked CXCR4 phosphorylation by VEGFR2 with vandetanib while also blocking SDF-1-mediated activation of CXCR4 using AMD3100 (Fig. 7E). Treatment with SSTN$_{VEGFR2}$ blocks VEGFR2 autophosphorylation and α4-S988 phosphorylation in NK cells or T cells plated on either VCAM-1 or mixed ICAM-1–VCAM-1 substrata (Fig. 7F). And under these conditions, which promote cell migration (see Fig. 7D), LFA-1 is observed to associate with VLA-4 in a single complex, shown by their co-immunoprecipitation (Fig. 7F). These findings suggest that the coupling of VEGFR2 to VLA-4 by Sdc1, and its stimulation of VLA-4 phosphorylation, prevent the VLA-4-mediated integrin transregulation of LFA-1 that NK cells and T cells need for their migration (see model, Fig. 7G) (Rose et al., 2003).

DISCUSSION

The capacity of VLA-4 to regulate cell migration and invasion is controlled by PKA-mediated phosphorylation of S988 in the cytoplasmic domain of its α4 integrin subunit (Goldfinger et al., 2003; Nishiya et al., 2005). Our work now demonstrates how this phosphorylation is accomplished, revealing a novel mechanism through which CXCR4, VEGFR2 and Sdc1 collaborate to regulate cell migration, with potentially broad implications for the roles of VLA-4, VEGFR2 and CXCR4 in the vascular, lymphatic and immune systems and in cancer. The two key features of this mechanism are (i) the VEGFR2 and VLA-4 docking site in the extracellular domain of Sdc1 that is active only when Sdc1 is cleaved and shed and can be inhibited by a peptide mimetic (SSTN$_{VEGFR2}$) (Jung et al., 2016), and (ii) a pre-assembled complex of CXCR4, PKA, AC7 and VEGFR2 that is necessary for PKA-mediated phosphorylation of VLA-4 and can be activated either by SDF-1 or by direct phosphorylation of CXCR4 by autophosphorylated VEGFR2, when VEGFR2 is coupled to active VLA-4 by sSdc1.

This represents one of several signaling mechanisms now described that are organized by docking sites in syndecan extracellular domains, including a second site in Sdc1 (amino acids 93–120) that organizes the type 1 insulin-like growth factor receptor (IGF1R) and the αvβ3 or αvβ5 integrins into a receptor complex that directs invasion and suppresses apoptosis in tumor cells and endothelial cells undergoing angiogenesis (Beauvais et al., 2009, 2016; Beauvais and Rapraeger, 2010). Additionally, a site in syndecan-4 (Sdc4) organizes the epidermal growth factor receptor (EGFR) and the α3β1 and α6β4 integrins into receptor complexes that stimulate cell migration and/or suppress stress signals (Beauvais et al., 2018 preprint; Wang et al., 2015). Unlike the other examples, however, the site in Sdc1 that couples VEGFR2 to VLA-4 is active only when the syndecan is shed (Jung et al., 2016). This implies an essential role for HPSE, which is known to activate MMP9-dependent shedding by trimming the HS chains on the syndecan (Yang et al., 2007), although how this activates shedding remains unknown.

The target of VEGFR2 kinase when CXCR4 is activated directly by tyrosine phosphorylation appears to be the highly conserved DRY motif found in the ∼700 members of the rhodopsin-like family of GPCRs (Fredriksson et al., 2003). This

Journal of Cell Science (2019) 132, jcs232645. doi:10.1242/jcs.232645

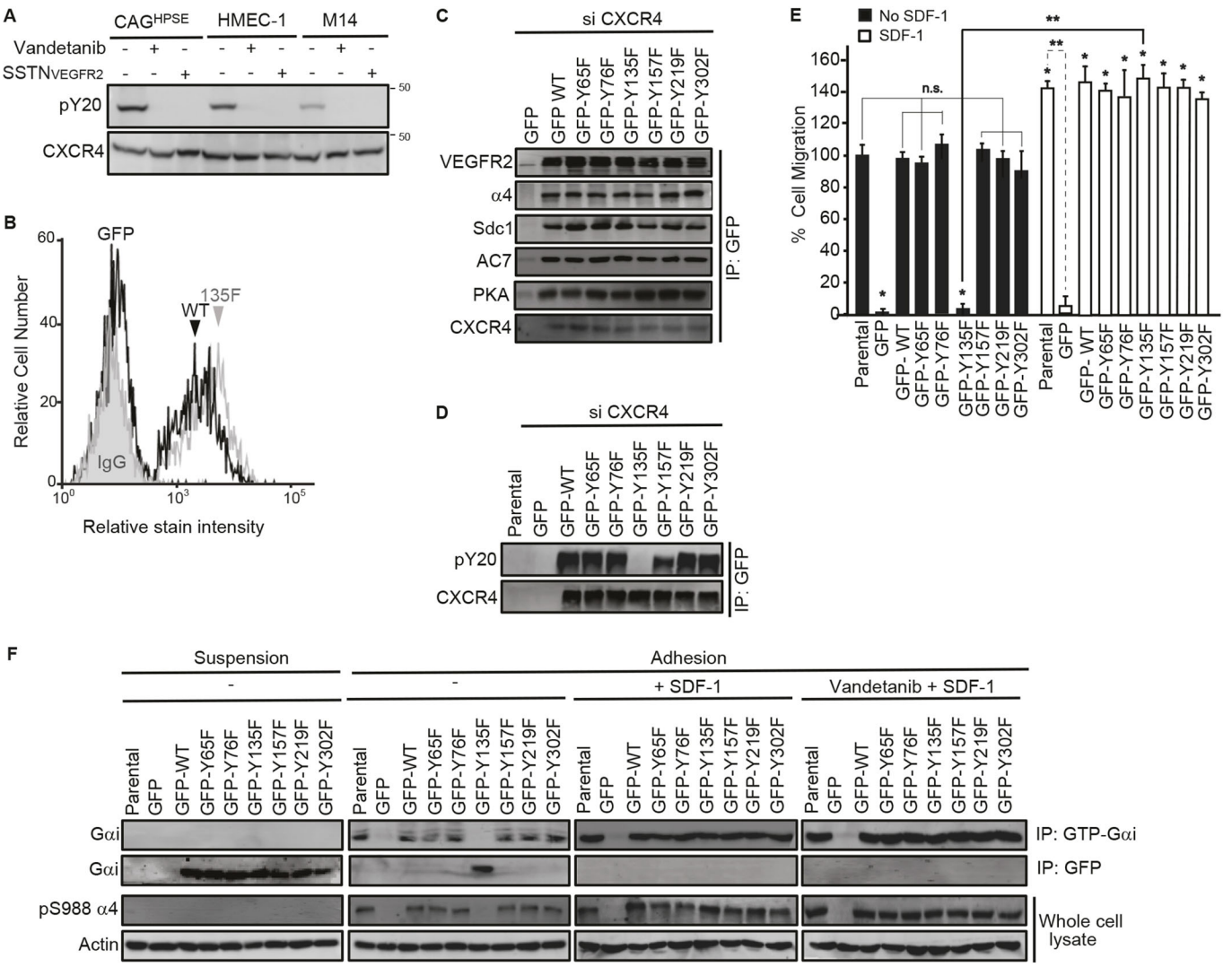

Fig. 5. VEGFR2 activates CXCR4 by phosphorylating Y135 in its DRY motif. (A) CAG^{HPSE}, HMEC-1 or M14 cells were plated on 100 µg/ml IIICS in the absence or presence of 10 µM vandetanib or 30 µM SSTN$_{VEGFR2}$ for 2.5 h. CXCR4 was immunoprecipitated with rabbit anti-CXCR4 antibody and the CXCR4-containing complexes were analyzed by immunoblotting with anti-phosphotyrosine or rat anti-CXCR4 antibody. (B–F) CAG^{HPSE}, HMEC-1 or M14 cells were co-transfected with CXCR4 3′UTR siRNA and CXCR4 cDNA lacking the 3′UTR (GFP-tagged WT and Y→F mutants or GFP alone) for 48 h. The cells were then analyzed by flow cytometry, immunoprecipitation and migration assays. (B) GFP-tagged WT or Y135F CXCR4 mutant HMEC-1 cells were incubated with PBS alone or 200 nM SDF-1 in PBS at 4°C. After incubation with 10 µg/ml anti-SDF-1 antibody versus an isotype-matched control mouse IgG1 for 1 h, cells were fixed and blocked with 3% BSA in PBS. The bound antibody was detected with a RPE-labeled anti-mouse IgG and analyzed by flow cytometry for SDF-1-bound CXCR4. (C) CAG^{HPSE} cell lysates were subjected to immunoprecipitation with anti-GFP antibody and then analyzed with anti-VEGFR2, anti-α4 integrin, anti-hSdc1, anti-AC7, anti-PKA or anti-CXCR4 antibodies. (D) M14 cell lysates were subjected to immunoprecipitation with anti-GFP antibody and then analyzed with anti-phosphotyrosine (pY20) or anti-CXCR4 antibodies. (E) Quantification of 16 h transfilter migration of CAG^{HPSE} cells towards 100 µg/ml IIICS in the absence or presence of 20 nM SDF-1 is plotted as the mean±s.d. of three independent experiments. All data were compared using the unpaired one-tailed *t*-test. **P*<0.01 against untreated parental cells; ***P*<0.01, n.s., not significant between treatments. (F) CAG^{HPSE} cells were kept in suspension or plated on 100 µg/ml IIICS in the absence or presence of 20 nM SDF-1 with or without 10 µM vandetanib for 2 h. Cell lysates were subjected to immunoprecipitation with anti-GFP or anti-GTP-Gα$_i$ antibodies, then probed with anti-Gα$_i$ antibody. The whole-cell lysates were analyzed by immunoblotting for integrin α4-pS988 and β-actin.

motif is one of several microswitches in CXCR4 thought to contribute to nucleotide exchange by Gα$_i$, although precisely how this occurs remains unknown owing to the lack of structural information on active CXCR4. Residues Y219 and Y302, found within the Y(x)$_5$KL microswitch in the cytoplasmic face of transmembrane domain 5 and the NPxxY motif located in transmembrane domain 7, respectively, form a ‘bridge’ with hydrophobic residue V242 in transmembrane domain 6. This provides the structural support for the direct binding of the Gα C-terminus with R134 in the DRY motif containing Y135 (Katritch et al., 2013; Wescott et al., 2016). This binding, along with Gα binding to Gβγ, stabilizes the association of the heterotrimeric G-protein with the GPCR, and at the same time locks GDP in the nucleotide-binding pocket to ‘prime’ the receptor for activation (Smrcka, 2008; Rasmussen et al., 2011). SDF-1 binding is postulated to re-orient these binding sites relative to Gα$_i$ and Gβγ, altering the interactions of switch I and II in Gα$_i$ with GDP and promoting exchange for GTP (Goncalves et al., 2010; Katritch et al., 2013; Wescott et al., 2016). This displaces Gα$_i$ and Gβγ from their respective binding sites on the receptor to independently affect downstream targets, such as AC7 by Gβγ (Oldham and Hamm, 2006; Smrcka, 2008).

Journal of Cell Science (2019) 132, jcs232645. doi:10.1242/jcs.232645

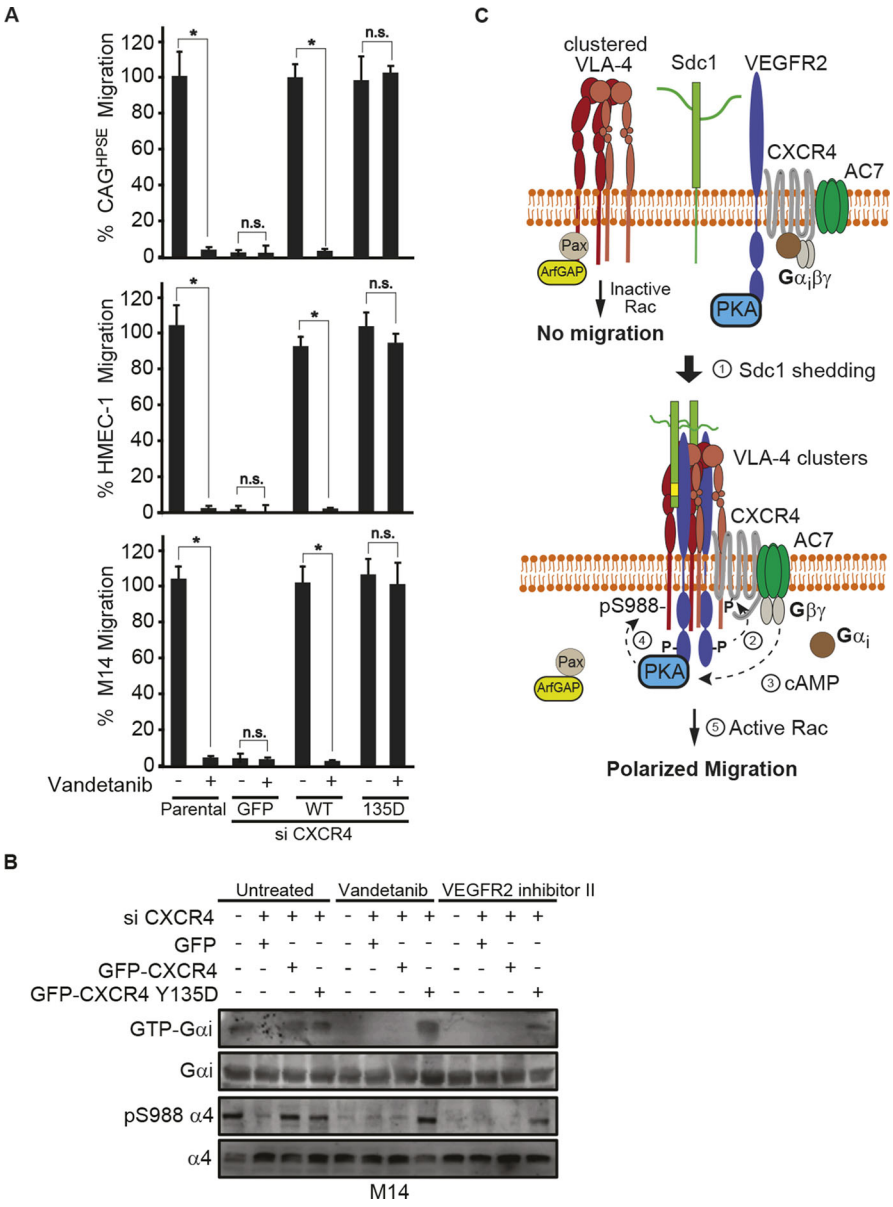

Fig. 6. The CXCR4 Y135D phosphomimetic mutant rescues the effects of VEGFR2 inhibition. (A,B) CAG^{HPSE}, HMEC-1 or M14 cells were transfected with GFP alone, GFP–CXCR4 WT, or GFP–CXCR4 Y135D together with siRNA targeting 3′UTR of endogenous CXCR4 for 48 h. (A) 16 h transfilter cell migration assay towards 100 µg/ml IIICS was performed in the absence or presence of 10 µM vandetanib. Migrated cells were quantified and graphed as the mean±s.d. from three independent experiments. All data were compared using the unpaired one-tailed *t*-test. **P*<0.01, n.s., not significant. (B) M14 cell lysates were subjected to immunoprecipitation with anti-GTP-Gα_i and probed for Gα_i. Whole-cell lysates were analyzed by immunoblotting for Gα_i or α4 integrin (total or pS988). (C) Model depicting how paxillin bound to VLA-4 causes inherent inhibition of Rac GTPase at this site due to its binding of ArfGAP (Nishiya et al., 2005). VEGFR2 forms a complex with CXCR4, AC7 and PKA, but this complex is inactive unless Sdc1 is shed. Trimming of the HS chains on Sdc1 by HPSE facilitates its shedding by MMP9 (Purushothaman et al., 2010; Yang et al., 2007). Sdc1 freed of its membrane anchorage couples VEGFR2 and its integrin phosphorylation machinery to VLA-4 clusters. VEGFR2 activated by this clustering event phosphorylates CXCR4 at Y135, activating its heterotrimeric G-protein. Gβγ freed of Gα_i activates AC7, generating cAMP that activates PKA. PKA phosphorylation of the α4 integrin cytoplasmic domain at S988 dissociates paxillin–ArfGAP from VLA-4, allowing local lamellipodium formation and directed cell migration.

The presence of tyrosines Y219, Y302 and Y135 in these microswitches make them potential candidates for regulating CXCR4 activation by tyrosine phosphorylation, although this has not been previously described. Our findings using myeloma, melanoma and endothelial cells strongly support the conclusion that Y135 is an important phosphorylation target, as VEGFR2-mediated activation is blocked by the Y135F mutation while mutation of the remaining cytoplasmic tyrosines is without effect. This mutation does not block G$\alpha_i\beta\gamma$ binding to CXCR4, nor does it have any effect on G-protein activation by SDF-1 binding to CXCR4, suggesting that phosphorylation of Y135 is specific for promoting GDP–GTP exchange and displacement of Gα_i and Gβγ from the receptor.

Although T cells and NK cells rely largely on LFA-1 for their influx to sites of inflammation or tumorigenesis (Chan et al., 2000; May et al., 2000; Rose et al., 2001), VLA-4 acts through ‘integrin transregulation’ to control this process (Alon et al., 1995; Chen et al., 1999; Ding et al., 2001). Transregulation depends on signaling from PYK2 and FAK kinases that are recruited to active VLA-4-bound paxillin (Rose et al., 2003). However, phosphorylation of S988 in the α4 integrin cytoplasmic domain displaces paxillin and prevents this transregulation (Cantor et al., 2015; Feral et al., 2006). Transregulation is enhanced in ITGA4-S988A mutant mice in which VLA-4 cannot be phosphorylated; such mice display enhanced LFA-1-dependent infiltration of cytotoxic T cells to B16 melanoma xenografts accompanied by reduced tumor growth (Cantor et al., 2015). As shown in this work, transregulation is also enhanced when VEGFR2 coupled to VLA-4 by shed Sdc1 is displaced by SSTN$_{VEGFR2}$, blocking the mechanism that causes integrin phosphorylation.

Although we have described this mechanism in tumor cell lines (melanoma and myeloma), it is well-known that HPSE (Kelly et al., 2003; Vornicova et al., 2016), VEGFR2 (Giatromanolaki et al., 2010; Mailankody et al., 2017; Molhoek et al., 2011), CXCR4 (Kim et al., 2006; Scala et al., 2005), VLA-4 (Mullen et al., 2008; Soodgupta et al., 2016) and Sdc1 (Maisnar et al., 2006; Orecchia et al., 2013) are expressed in individuals with melanoma and myeloma, supporting the clinical relevance of our findings.

Journal of Cell Science (2019) 132, jcs232645. doi:10.1242/jcs.232645

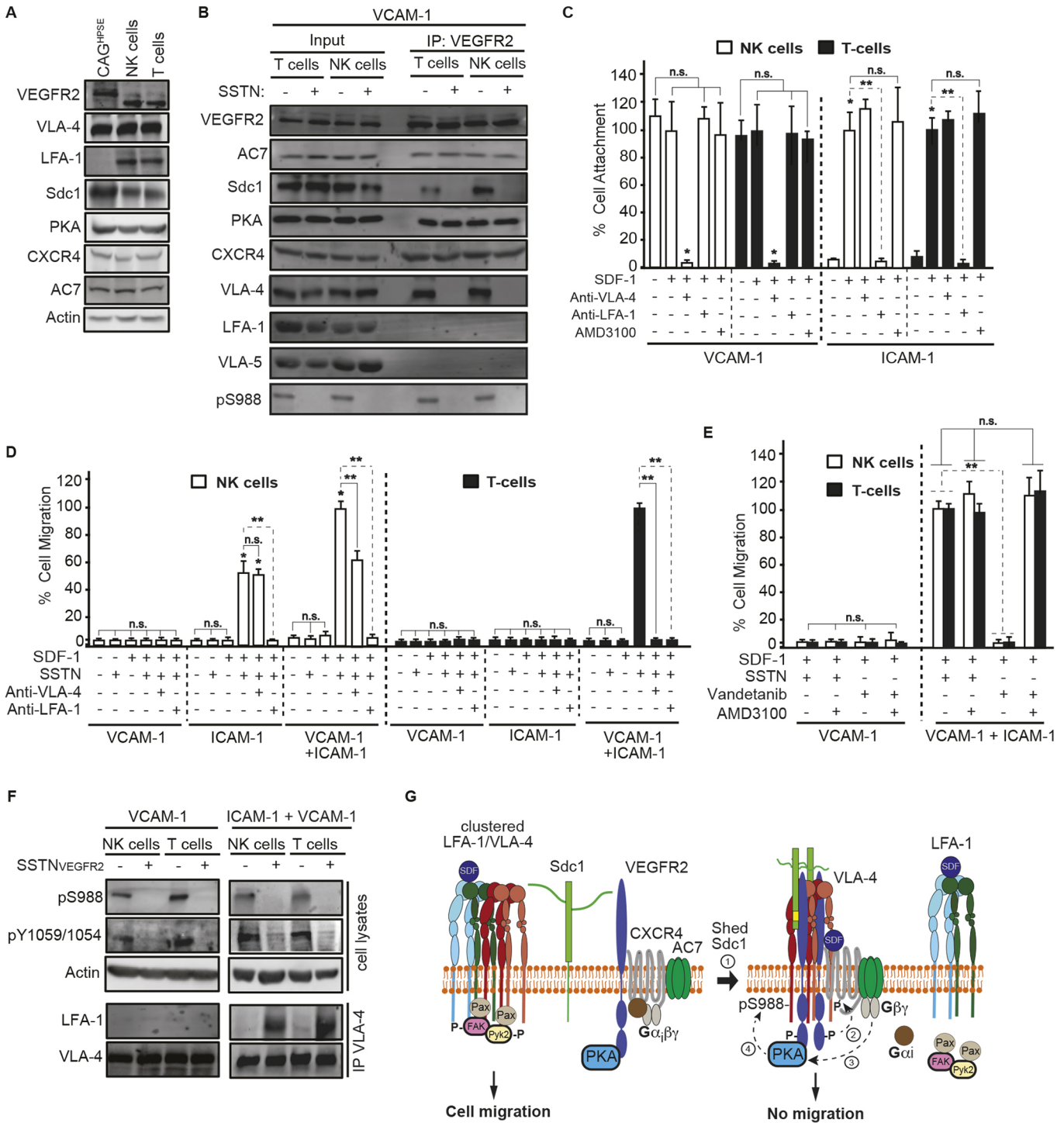

Fig. 7. See next page for legend.

Prior studies describing VLA-4 phosphorylation were conducted in human microvascular endothelial cells (Goldfinger et al., 2008), mouse primary T cells (Cantor et al., 2015; Hyduk et al., 2004), lymphoma cells including Jurkat (T lymphoma), Hut78 (T lymphoma), CCRF CEM (T lymphoma) and U-937 (myeloid-derived lymphoma), and leukemia (THP-1) cells (Han et al., 2003; Hyduk et al., 2004). Although a role for VEGFR2 was not described at the time, our work suggests that it is likely to be involved. We show here that representative HMEC-1 endothelial cells and primary mouse T cells rely on VEGFR2 coupled to VLA-4 by Sdc1. With regard to lymphoma, we have examined a representative T lymphoma cell line (Jurkat) and find VEGFR2 inhibitors or $SSTN_{VEGFR2}$ blocks α4 integrin phosphorylation in these cells as well (data not shown). Although we have not tested the U-937 and THP-1 cells, they are known to express VEGFR2 (Jankowski et al., 2013; Kaur et al., 2014; Nóbrega-Pereira et al., 2018; Wheeler et al., 2018). Furthermore, clinical studies show that VEGFR2 is expressed in more than 90% of individuals with Hodgkin lymphoma (Dimtsas et al., 2014), non-Hodgkin lymphoma (Stopeck et al., 2009) and leukemia (Ferrajoli et al., 2001).

Journal of Cell Science

Fig. 7. sSdc1-mediated VEGFR2 activation suppresses cytotoxic T cell and NK cell migration by displacing VLA-4 from LFA-1. (A) Lysates from CAG^{HPSE} cells, NK cells and T cells were analyzed by immunoblotting for VEGFR2, VLA-4, LFA-1, Sdc1, PKA, CXCR4, AC7 and β-actin (loading control). (B) NK cells and T cells were plated on 10 µg/ml VCAM-1 in the absence or presence of 30 µM $SSTN_{VEGFR2}$ for 2.5 h. VEGFR2 was immunoprecipitated and the VEGFR2-containing complexes analyzed by immunoblotting for VEGFR2, AC7, Sdc1, PKA, CXCR4, α4 integrin [total (VLA-4) and pS988], LFA-1 and VLA-5. (C) NK cells and T cells were plated on either ICAM-1 or VCAM-1 in the absence or presence of SDF-1 with or without anti-VLA-4 or anti-LFA-1 antibodies or CXCR4 inhibitor (AMD3100). Attached NK cells and T cells in five random images for each experiment were quantified and graphed as a percent of cells treated with SDF-1 alone (set to 100%). All data were compared using the unpaired one-tailed *t*-test. **P*<0.01 against untreated parental cells; ***P*<0.01, n.s., not significant between treatments. (D) 16 h transfilter cell migration assays towards 10 µg/ml VCAM-1 alone, 10 µg/ml ICAM-1 alone, or a mixture of 10 µg/ml ICAM-1 with 10 µg/ml VCAM-1, analysis after treatment with 30 µM $SSTN_{VEGFR2}$, 10 µg/ml anti-VLA-4, or 10 µg/ml anti-LFA-1 in the absence or presence of SDF-1. Migrated cells were quantified and graphed as the mean±s.d. from three independent experiments. All data were compared using the unpaired one-tailed *t*-test. **P*<0.01 against untreated parental cells on each ligand; ***P*<0.01, n.s., not significant between treatments. (E) 16 h transfilter cell migration assays towards 10 µg/ml VCAM-1 alone or mixture of 10 µg/ml ICAM-1 plus 10 µg/ml VCAM-1 was performed as in D in the absence or presence of 30 µM $SSTN_{VEGFR2}$, 1 µM vandetanib or 10 µM AMD3100. All data were compared using the unpaired one-tailed *t*-test. ***P*<0.01, n.s., not significant. (F) NK cells and T cells were plated on 10 µg/ml VCAM-1 alone or mixture of 10 µg/ml ICAM-1 with 10 µg/ml VCAM-1 in the absence or presence of $SSTN_{VEGFR2}$. Cell lysates were subjected to immunoprecipitation of VLA-4 and probed for VLA-4 or LFA-1. Whole-cell lysates were analyzed by immunoblotting for integrin α4-pS988, VEGFR2-pY1054/1059 or β-actin. (G) Model depicting how LFA-1 and VLA-4 on NK cells and T cells associate in an adhesion complex in which signaling from FAK and PYK2, localized to VLA-4 by paxillin, transregulates LFA-1 activity leading to LFA-1-dependent cell migration (Cantor et al., 2015; Rose et al., 2003). If Sdc1 is shed by the leukocytes, or high levels of shed Sdc1 accumulate in the tumor microenvironment from HPSE-overexpressing tumor cells, the shed syndecan couples VEGFR2 and its phosphorylation machinery to VLA-4. Activation of CXCR4 by SDF-1, or by VEGFR2-mediated phosphorylation of Y135 in the CXCR4 cytoplasmic loop 2, causes phosphorylation of S988 in the α4 integrin subunit, displacing paxillin and suppressing LFA-1-mediated influx of cytotoxic leukocytes to the tumor. $SSTN_{VEGFR2}$, which reverses the effects of shed syndecan, relieves this immunosuppression while at the same time blocking tumor cell migration and metastasis (see Fig. 6C).

We speculate that shed Sdc1 generated by HPSE-expressing tumor cells, shown for malignant multiple myeloma where high levels of shed Sdc1 accumulate in the bone marrow and plasma of individuals with myeloma (Dhodapkar et al., 1997), acts as an autocrine factor in the tumor microenvironment to stimulate tumor cell migration and angiogenesis, and as a novel paracrine immune suppression mechanism, thereby promoting the extravasation and survival of these malignancies.

MATERIALS AND METHODS

Reagents

HPSE inhibitor OGT2115 is from TOCRIS Bioscience (Minneapolis, MN). $SSTN_{VEGFR2}$ peptide (ETSGENTAVVAVEPDRRNQSPVD) and $SSTN_{IGF1R}$ (STSTLPAGEGPKEGEAVVLPEVEPGLTAR) are provided by LifeTein (Plainfield, NJ) as HCl salts and dissolved as 100× stock in 50 mM HEPES-buffered (pH 7.4) Dulbecco's modified Eagle's medium. Vandetanib (ZD6474) is from LC Laboratories (Woburn, MA). Rat [mAb 2B11, 14-9991-82; 1:1000 for immunoblotting (IB)], mouse (mAb 12G5, 555972; 1:50 to block SDF-1 binding) and rabbit [AB1846; 1:100 for immunoprecipitation (IP)] anti-CXCR4 antibodies are from eBioscience (San Diego, CA), BD Biosciences (San Diego, CA) and Millipore-Sigma (Burlington, MA), respectively. Rabbit polyclonal anti-α4 integrin (PA5-20600; 1:1000 for IB), anti-pY1054/1059 VEGFR2 (44-1047G; 1:1000 for IB), anti-CXCR3 (PA5-28741; 1:1000 for IB) and mouse anti-LFA-1 (mAb TS1/22,MA11A10; 1:400 for IB) are from Thermo Fisher Scientific (Grand Island, NY). Anti-α4 integrin mouse monoclonals P1H4 (MAB16983Z; 1:1000 for IB), HP2/1 (MAB1383; 1:1000 for IB), rabbit anti-pS988 α4 integrin (AB1919; 1:2000 for IB), anti-integrin α5 (MABT201; 1:1000 for IB), mouse anti-VEGFR2 (mAb CH-11, 05-554; 1:1000 for IB) and anti-β-actin (mAb AC-74, A-5316; 1:2000 for IB), selective PKA activator 6-Bnz-cAMP (116802), PKA inhibitor H-89 (371962), pertussis toxin (516561), VEGFR2 kinase inhibitor II (676485) and forskolin (F-6886) are all from Millipore-Sigma. Anti-PKA (4782S; 1:2000), anti-VEGFR2 (mAb 55B11; 2479S; 1:1000 for IB, 1:200 for IP), anti-cytoSdc1 (12922S; 1:1000 for IB) and anti-$G\alpha_i$ (5290S; 1:1000 for IB) antibodies are from Cell Signaling Technology (Danver, MA). Anti-pT197 PKA (mAb EP2606Y, ab75991; 1:2000 for IB) antibody and CXCR4 antagonist AMD3100 (ab120718) are from Abcam (Cambridge, MA). Gallein inhibitor (sc-202631), anti-Gβγ (mAb M-14, sc-261; 1:1000 for IB) and anti-human AC7 (clone H-120, sc-25501; 1:1000 for IB) antibodies are from Santa Cruz Biotechnology (Santa Cruz, CA). Anti-GTP-$G\alpha_i$ (26901; 1:1000 for IP) antibody is from NewEast Biosciences (King of Prussia, PA). Anti-AC2 (NBP1-33659; 1: 1000 for IB) and anti-α4 integrin (mAb 2C11, H00003676-M01; 1:1000 for IB) antibodies are from Novus Biologicals (Centennial, CO). Anti-AC4 (LS-C200088; 1:1000 for IB) and anti-AC7 (LS-C156070; 1:1000 for IB) antibodies are from LifeSpan BioSciences (Seattle, WA). Anti-phosphotyrosine (mAb pY20, P11120; 1:2000 for IB) antibody is from BD Biosciences. Recombinant human SDF-1α (300-28A) is from Peprotech (Rocky Hill, NJ). Anti-SDF-1 (clone 79018; 0.25 µg/million cells) antibody was from R&D Systems (Minneapolis, MN). Anti-GFP antibody was kindly provided by Dr Larry Delucas (The University of Alabama at Birmingham, AL, USA). Polyclonal antibodies against human Sdc1 (1 µg/ml) (Beauvais et al., 2004) and monoclonal anti-mSdc1 281.2 (1 µg/ml) (Jung et al., 2016) were described previously. Anti-human Sdc1 (mAb B-A38; 1:1000) antibody is from Acris Antibodies (San Diego, CA). Alkaline phosphatase (AP)-conjugated goat anti-rat IgG (112-055-003; 1:5000), AP-conjugated goat anti-mouse IgG (115-055-146; 1:5000), and AP-conjugated goat anti-rabbit IgG (111-055-003; 1:5000) are from Jackson ImmunoResearch (West Grove, PA). Goat anti-mouse IgG (H+L) cross-adsorbed RPhycoerythrin (R-PE) secondary antibody (P-892; 1 µg/ml) and Alexa Fluor 546 phalloidin (A22283; 1:200) are from Molecular Probes (Eugene, OR).

Complementary DNA

Mutant CXCR4 cDNA was prepared by PCR using hCXCR4 VersaClone cDNA obtained through R&D Systems (RDC0032) as a template. One primer (5′-TCAAGTTTTCACTCCAGCAAACCGGTAGGCGCGCCAG TATAC-3′) was used to add an AgeI enzyme site at the 5′ end of CXCR4 and another (5′-GTATACTGGCGCGCCTACCGGTTTGCTGGAGTGA AAACTTGA-3′) to delete a stop codon at the 3′ end of the CXCR4 gene. The PCR fragment obtained with this primer pair was then subcloned into the pEGFP-N1 expression vector (EGFP-CXCR4 WT) and this construct was used as a template for the construction of tyrosine point mutants using the following primers: Y65F (5′-CTGGTCATGGGTTTCCAGAAGAA ACTG-3′), Y76F (5′-ATGACGGACAAGTTCAGGCTGCACCTG-3′), Y135F (5′-AGTCTGGACCGCTTCCTGGCCATCGTC-3′), 135D (5′-A GTCTGGACCGCGACCTGGCCATCGTC-3′), Y157F (5′-GAAAAGG TGGTCTTTGTTGGCGTCTGG-3′), Y219F (5′-ATCCTGTCCTGC TTTTGCATTATCATC-3′) and Y302F (5′-AACCCCATCCTCTTTGCT TTCCTTGGA-3′). An N-terminal HA-tag was added (using PCR primer 5′-GAG ATC GAA TTC CGG GCC GCT TAG TGT TGA ATG TAC CCA TAC GAC GTC CCA GAC TAC GCT ATG TTC CCC ACC GAG AGC GCA TGG CTT GGG AAG-3′, HA sequence underlined) to α4 integrin WT and mutants (S988A and S988D) pcDNA 3.0 expression constructs kindly provided by Dr Mark Ginsberg (UCSD). All constructs were confirmed by sequencing prior to use.

Transfection

The expression of Sdc1 in the pcDNA3 vector was previously described (Jung et al., 2016). Small interfering RNAs specific for human Sdc1 (hSdc1 siRNA #2, 5′-GGAGGAATTCTATGCCTGA-3′ and hSdc1 siRNA #1,

5′-AAGGAGGAATTCTATGCCTGA-3′), α4 integrin siRNA (5′-CAGA CTCAGGTTGTAGTAAAGAAA-3′), AC2 siRNA (5′-GAACCAAGTC ACAAAAGGAA-3′), AC4 siRNA (5′-CAATTTCCACAGCCTCTAT-3′), AC7 siRNA (5′-CGATGACTTCTACACCTTT-3′), CXCR4 siRNA #1 (5′-CCAAGATGTGACTTTGAAA-3′), CXCR4 siRNA #2 (5′-GCC AAGATGTGACTTTGAA-3′) and CXCR3 siRNA (5′-GGACTTGAGCC TGAACTTCTT-3′) were designed and provided by Ambion (Austin, TX). VEGFR2 siRNA (5′-AAGGCTAATACAACTCTTCAA-3′) was designed and provided by Qiagen (Chatsworth, CA). For transfection, 60 pmol siRNA or 5 µg of DNA was added to 10^6 cells in six-well plates using Lipofectamine 2000 and Opti-MEM transfection medium (Invitrogen, Carlsbad, CA) lacking serum and antibiotics, followed by 3 ml complete growth medium after 5 h.

Cell adhesion assay

The derivation and culture of CAG^{HPSE} myeloma and HMEC-1 have been previously described (Beauvais et al., 2004; Jung et al., 2016). M14 cells were kindly provided by Dr David Cheresh (University of California San Diego, CA, USA). Cells were short tandem repeat-profiled for cell identification and tested routinely to ensure they were free from mycoplasma. Nitrocellulose-treated slides were coated for 2 h at 37°C with 40 µg/ml FN (kindly provided by Dr Donna Peters, University of Wisconsin-Madison, USA), 100 µg/ml GST-IIICS FN fragment (prepared as described in Jung et al., 2016), 10 µg/ml of VCAM-1 or 10 µg/ml of ICAM-1 (R&D Systems) in calcium- and magnesium-free PBS (CMF-PBS; 135 mM NaCl, 2.7 mM KCl, 10.2 mM Na_2HPO_4-$7H_20$ and 1.75 mM KH_2PO_4, pH 7.4), followed by blocking with RPMI 1640 containing 1% heat-denatured BSA (plating medium). Cells in plating medium were allowed to attach and spread for 2.5 h at 37°C, then were fixed in 4% electron microscopy (EM)-grade paraformaldehyde (Electron Microscopy Sciences, Hatfield, PA) in CMF-PBS and labeled for 30 min in 0.13 µM rhodamine phalloidin (Invitrogen) or 2 µM Hoechst 33342 (AdipoGen Life Sciences, San Diego, CA). Cells were imaged with a Nikon Microphot FX microscope using a 20× objective (Nikon; Ex 541-551, DM 580, Barrier 590), Photometric CoolSnap ES camera, and version 7.7.3.0 Metamorph Imaging software (Molecular Devices, San Jose, CA). All images represent results from triplicate wells and three independent experiments.

Migration assay

The bottom surface of Transwell filters (8 µm pores for CAG^{HPSE}, HMEC-1 or M14 cells; 3 µm pores for T cells and NK cells; Corning Life Sciences, Corning, NY) were coated with 40 µg/ml of FN, 100 µg/ml of GST-IIICS (prepared as described in Jung et al., 2016), 10 µg/ml of VCAM-1, 10 µg/ml of ICAM-1, or a mixture of 10 µg/ml of VCAM-1 and 10 µg/ml of ICAM-1. CAG^{HPSE} (5×10^5), HMEC-1 (5×10^4), M14 (5×10^4), T cells or NK cells (1×10^7) were placed in the upper chamber with or without indicated inhibitors and incubated for 16 h at 37°C. Cells on the bottom of the filter were fixed with 4% paraformaldehyde diluted in CMF-PBS and stained with 0.1% Crystal Violet, and five random fields were imaged and counted. Statistical analysis was performed using data from at least three independent experiments.

Immunoprecipitation and immunoblotting

Cells were lysed in ice-cold buffer containing 0.5% Triton X-100, 50 mM HEPES (pH 7.4), 50 mM NaCl 10 mM EDTA and 1:1000 protease inhibitor cocktail III (Millipore-Sigma). Cell lysates were collected and analyzed on western blots as described (Jung et al., 2016). Bands were detected with AP-conjugated antibody and ECF reagent (GE Healthcare Biosciences, Pittsburgh, PA) on a Typhoon Trio Variable Mode Imager (GE Healthcare). For immunoprecipitation, 1 mg of protein was incubated at 4°C overnight with 1 µg of specific antibody or non-specific mouse IgG. After washing four times with lysis buffer, the protein complex was dissolved in SDS Laemmli sample buffer containing 62.5 mM Tris (pH 6.8), 2.5% SDS, 0.002% Bromophenol Blue, 10% glycerol and 5% β-mercaptoethanol. For immunoblotting, 20 µg of protein samples were loaded and analyzed on western blots as described (Jung et al., 2016). All images represent results from three independent experiments.

Flow cytometry

To measure the amount of GFP-tagged CXCR4 expressed on the surface of transfected HMEC-1 cells, 1×10^6 cells were incubated in 30 µl PBS for 1 h at 4°C to prevent subsequent internalization, and 30 µl of 200 nM SDF-1α solution was then added and incubated for 20 min at 4°C after cell centrifugation. After washing with PBS, cells were fixed in 4% EM-grade paraformaldehyde and 30 µl anti-SDF-1 antibody at 10 µg/ml was added for 30 min, and bound antibody was revealed by addition of 50 µl of RPE secondary immunoglobulin (Molecular Probes, P-892; 1 µg/ml). After 30 min staining, cells were washed with PBS and then were subjected to flow cytometry to assess relative levels of bound SDF-1.

T cell and NK cell preparation

T cells and NK cells from spleens of adult C57BL/6 mice (10–12 weeks) were isolated via negative depletion with the use of a magnetic bead selection kit [mouse NK (130-096-892) or T cell (130-095-130) isolation kit (Miltenyi Biotec, Bergisch Gladbach, Germany] according to the manufacturer's protocol. All animal use was conducted after prior approval by the University of Wisconsin-Madison Institutional Animal Care and Use Committee.

Acknowledgements

We thank Dr Mark Ginsberg, University of California-San Diego, USA, for the kind gift of the ITGA4 WT, S988A and S988D cDNA constructs. Dr Christian Capitini (University of Wisconsin-Madison, USA) and members of his laboratory are thanked for assistance in isolating NK cells and T cells.

Competing interests

The authors declare no competing or financial interests.

Author contributions

Conceptualization: O.J., D.M.B., A.C.R.; Methodology: O.J.; Formal analysis: O.J.; Investigation: O.J., K.M.A.; Data curation: O.J.; Writing - original draft: O.J., A.C.R.; Writing - review & editing: D.M.B., K.M.A., A.C.R.; Supervision: A.C.R.; Project administration: A.C.R.; Funding acquisition: A.C.R.

Funding

This work was supported by funds from the National Institutes of Health to A.C.R. (R01-CA139872, R01-CA212413), a fellowship to O.J. from the American Heart Association, funds from the University of Wisconsin Carbone Cancer Center's Trillium Fund, and the use of its shared services, supported by NIH/NCI P30 CA014520. Deposited in PMC for release after 12 months.

Supplementary information

Supplementary information available online at
http://jcs.biologists.org/lookup/doi/10.1242/jcs.232645.supplemental

References

Alon, R., Kassner, P. D., Carr, M. W., Finger, E. B., Hemler, M. E. and Springer, T. A. (1995). The integrin VLA-4 supports tethering and rolling in flow on VCAM-1. *J. Cell Biol.* **128**, 1243-1253. doi:10.1083/jcb.128.6.1243

Audet, M. and Bouvier, M. (2012). Restructuring G-protein- coupled receptor activation. *Cell* **151**, 14-23. doi:10.1016/j.cell.2012.09.003

Balkwill, F. (2004). The significance of cancer cell expression of the chemokine receptor CXCR4. *Semin. Cancer Biol.* **14**, 171-179. doi:10.1016/j.semcancer.2003.10.003

Beauvais, D. M. and Rapraeger, A. C. (2010). Syndecan-1 couples the insulin-like growth factor-1 receptor to inside-out integrin activation. *J. Cell Sci.* **123**, 3796-3807. doi:10.1242/jcs.067645

Beauvais, D. L. M., Burbach, B. J. and Rapraeger, A. C. (2004). The syndecan-1 ectodomain regulates αvβ3 integrin activity in human mammary carcinoma cells. *J. Cell Biol.* **167**, 171-181. doi:10.1083/jcb.200404171

Beauvais, D. L. M., Ell, B. J., McWhorter, A. R. and Rapraeger, A. C. (2009). Syndecan-1 regulates αvβ3 and αvβ5 integrin activation during angiogenesis and is blocked by synstatin, a novel peptide inhibitor. *J. Exp. Med.* **206**, 691-705. doi:10.1084/jem.20081278

Beauvais, D. M., Jung, O., Yang, Y., Sanderson, R. D. and Rapraeger, A. C. (2016). Syndecan-1 (CD138) suppresses apoptosis in multiple myeloma by activating IGF1 receptor: prevention by synstatinIGF1R inhibits tumor growth. *Cancer Res.* **76**, 4981-4993. doi:10.1158/0008-5472.CAN-16-0232

Beauvais, D. M., Short, K., Stueven, N., Nelson, S. E., Lee, D., Jung, O., Anderson, R. A., Lambert, P. F. and Rapraeger, A. C. (2018). MST1R/RON and

EGFR in a complex with syndecans sustain carcinoma S-phase progression by preventing p38MAPK activation. *bioRxiv* 252742. doi:10.1101/252742

Blanco, R. and Gerhardt, H. (2013). VEGF and Notch in tip and stalk cell selection. *Cold Spring Harb. Perspect Med.* **3**, a006569. doi:10.1101/cshperspect.a006569

Cantor, J. M., Rose, D. M., Slepak, M. and Ginsberg, M. H. (2015). Fine-tuning tumor immunity with integrin trans-regulation. *Cancer Immunol. Res.* **3**, 661-667. doi:10.1158/2326-6066.CIR-13-0226

Chan, J. R., Hyduk, S. J. and Cybulsky, M. I. (2000). α4β1 integrin/VCAM-1 interaction activates αLβ2 integrin-mediated adhesion to ICAM-1 in human T cells. *J. Immunol.* **164**, 746-753. doi:10.4049/jimmunol.164.2.746

Chen, C., Mobley, J. L., Dwir, O., Shimron, F., Grabovsky, V., Lobb, R. R., Shimizu, Y. and Alon, R. (1999). High affinity very late antigen-4 subsets expressed on T cells are mandatory for spontaneous adhesion strengthening but not for rolling on VCAM-1 in shear flow. *J. Immunol.* **162**, 1084-1095.

Dhodapkar, M. V., Kelly, T., Theus, A., Athota, A. B., Barlogie, B. and Sanderson, R. D. (1997). Elevated levels of shed syndecan-1 correlate with tumour mass and decreased matrix metalloproteinase-9 activity in the serum of patients with multiple myeloma. *Br. J. Haematol.* **99**, 368-371. doi:10.1046/j.1365-2141.1997.3893203.x

Dimtsas, G. S., Georgiadi, E. C., Karakitsos, P., Vassilakopoulos, T. P., Thymara, I., Korkolopoulou, P., Patsouris, E., Kittas, C. and Doussis-Anagnostopoulou, I. A. (2014). Prognostic significance of immunohistochemical expression of the angiogenic molecules vascular endothelial growth factor-A, vascular endothelial growth factor receptor-1 and vascular endothelial growth factor receptor-2 in patients with classical Hodgkin lymphoma. *Leuk. Lymphoma* **55**, 558-564. doi:10.3109/10428194.2013.813629

Ding, Z., Xiong, K. and Issekutz, T. B. (2001). Chemokines stimulate human T lymphocyte transendothelial migration to utilize VLA-4 in addition to LFA-1. *J. Leukoc. Biol.* **69**, 458-466. doi:10.1189/jlb.69.3.458

Fearon, D. T. (2016). Explaining the paucity of intratumoral T cells: a construction out of known entities. *Cold Spring Harb. Symp. Quant. Biol.* **81**, 219-226. doi:10.1101/sqb.2016.81.030783

Feral, C. C., Rose, D. M., Han, J., Fox, N., Silverman, G. J., Kaushansky, K. and Ginsberg, M. H. (2006). Blocking the α4 integrin-paxillin interaction selectively impairs mononuclear leukocyte recruitment to an inflammatory site. *J. Clin. Invest.* **116**, 715-723. doi:10.1172/JCI26091

Ferrajoli, A., Manshouri, T., Estrov, Z., Keating, M. J., O'Brien, S., Lerner, S., Beran, M., Kantarjian, H. M., Freireich, E. J. and Albitar, M. (2001). High levels of vascular endothelial growth factor receptor-2 correlate with shortened survival in chronic lymphocytic leukemia. *Clin. Cancer Res.* **7**, 795-799.

Fredriksson, R., Lagerstrom, M. C., Lundin, L. G. and Schioth, H. B. (2003). The G-protein-coupled receptors in the human genome form five main families. Phylogenetic analysis, paralogon groups, and fingerprints. *Mol. Pharmacol.* **63**, 1256-1272. doi:10.1124/mol.63.6.1256

Garmy-Susini, B., Avraamides, C. J., Schmid, M. C., Foubert, P., Ellies, L. G., Barnes, L., Feral, C., Papayannopoulou, T., Lowy, A., Blair, S. L. et al. (2010). Integrin α4β1 signaling is required for lymphangiogenesis and tumor metastasis. *Cancer Res.* **70**, 3042-3051. doi:10.1158/0008-5472.CAN-09-3761

Gavalas, N. G., Tsiatas, M., Tsitsilonis, O., Politi, E., Ioannou, K., Ziogas, A. C., Rodolakis, A., Vlahos, G., Thomakos, N., Haidopoulos, D. et al. (2012). VEGF directly suppresses activation of T cells from ascites secondary to ovarian cancer via VEGF receptor type 2. *Br. J. Cancer* **107**, 1869-1875. doi:10.1038/bjc.2012.468

Giatromanolaki, A., Bai, M., Margaritis, D., Bourantas, K. L., Koukourakis, M. I., Sivridis, E. and Gatter, K. C. (2010). Hypoxia and activated VEGF/receptor pathway in multiple myeloma. *Anticancer Res.* **30**, 2831-2836.

Goel, H. L. and Mercurio, A. M. (2013). VEGF targets the tumour cell. *Nat. Rev. Cancer* **13**, 871-882. doi:10.1038/nrc3627

Goldfinger, L. E., Han, J., Kiosses, W. B., Howe, A. K. and Ginsberg, M. H. (2003). Spatial restriction of α4 integrin phosphorylation regulates lamellipodial stability and α4β1-dependent cell migration. *J. Cell Biol.* **162**, 731-741. doi:10.1083/jcb.200304031

Goldfinger, L. E., Tzima, E., Stockton, R., Kiosses, W. B., Kinbara, K., Tkachenko, E., Gutierrez, E., Groisman, A., Nguyen, P., Chien, S. et al. (2008). Localized α4 integrin phosphorylation directs shear stress-induced endothelial cell alignment. *Circ. Res.* **103**, 177-185. doi:10.1161/CIRCRESAHA.108.176354

Goncalves, J. A., South, K., Ahuja, S., Zaitseva, E., Opefi, C. A., Eilers, M., Vogel, R., Reeves, P. J. and Smith, S. O. (2010). Highly conserved tyrosine stabilizes the active state of rhodopsin. *Proc. Natl. Acad. Sci. USA* **107**, 19861-19866. doi:10.1073/pnas.1009405107

Guerin, E., Sheridan, C., Assheton, D., Kent, D., Wong, D., Grant, M. and Hiscott, P. (2008). SDF1-α is associated with VEGFR-2 in human choroidal neovascularisation. *Microvasc. Res.* **75**, 302-307. doi:10.1016/j.mvr.2007.12.001

Han, J., Rose, D. M., Woodside, D. G., Goldfinger, L. E. and Ginsberg, M. H. (2003). Integrin α4β1-dependent T cell migration requires both phosphorylation and dephosphorylation of the α4 cytoplasmic domain to regulate the reversible binding of paxillin. *J. Biol. Chem.* **278**, 34845-34853. doi:10.1074/jbc.M304691200

Han, A.-R., Lee, J. Y., Kim, H.-J., Min, W. S., Park, G. and Kim, S.-H. (2015). A CXCR4 antagonist leads to tumor suppression by activation of immune cells in a leukemia-induced microenvironment. *Oncol. Rep.* **34**, 2880-2888. doi:10.3892/or.2015.4297

Hemler, M. E., Elices, M. J., Parker, C. and Takada, Y. (1990). Structure of the integrin VLA-4 and its cell-cell and cell-matrix adhesion functions. *Immunol. Rev.* **114**, 45-65. doi:10.1111/j.1600-065X.1990.tb00561.x

Hofer, A. M. and Lefkimmiatis, K. (2007). Extracellular calcium and cAMP: second messengers as "third messengers"? *Physiology (Bethesda)* **22**, 320-327. doi:10.1152/physiol.00019.2007

Horikawa, N., Abiko, K., Matsumura, N., Hamanishi, J., Baba, T., Yamaguchi, K., Yoshioka, Y., Koshiyama, M. and Konishi, I. (2017). Expression of vascular endothelial growth factor in ovarian cancer inhibits tumor immunity through the accumulation of myeloid-derived suppressor cells. *Clin. Cancer Res.* **23**, 587-599. doi:10.1158/1078-0432.CCR-16-0387

Hyduk, S. J., Oh, J., Xiao, H., Chen, M. and Cybulsky, M. I. (2004). Paxillin selectively associates with constitutive and chemoattractant-induced high-affinity α4β1 integrins: implications for integrin signaling. *Blood* **104**, 2818-2824. doi:10.1182/blood-2003-12-4402

Jach, R., Dulinska-Litewka, J., Laidler, P., Szczudrawa, A., Kopera, A., Szczudlik, L., Pawlik, M., Zajac, K., Mak, M. and Basta, A. (2010). Expression of VEGF, VEGF-C and VEGFR-2 in in situ and invasive SCC of cervix. *Front. Biosci. (Elite Ed)* **2**, 411-423. doi:10.2741/e101

Jankowski, V., Schulz, A., Kretschmer, A., Mischak, H., Boehringer, F., van der Giet, M., Janke, D., Schuchardt, M., Herwig, R., Zidek, W. et al. (2013). The enzymatic activity of the VEGFR2 receptor for the biosynthesis of dinucleoside polyphosphates. *J. Mol. Med. (Berl.)* **91**, 1095-1107. doi:10.1007/s00109-013-1036-y

Jin, H., Su, J., Garmy-Susini, B., Kleeman, J. and Varner, J. (2006). Integrin α4β1 promotes monocyte trafficking and angiogenesis in tumors. *Cancer Res.* **66**, 2146-2152. doi:10.1158/0008-5472.CAN-05-2704

Juneja, H. S., Schmalsteig, F. C., Lee, S. and Chen, J. (1993). Vascular cell adhesion molecule-1 and VLA-4 are obligatory adhesion proteins in the heterotypic adherence between human leukemia/lymphoma cells and marrow stromal cells. *Exp. Hematol.* **21**, 444-450. doi:10.1016/s0145-2126(98)00070-8

Jung, O., Trapp-Stamborski, V., Purushothaman, A., Jin, H., Wang, H., Sanderson, R. D. and Rapraeger, A. C. (2016). Heparanase-induced shedding of syndecan-1/CD138 in myeloma and endothelial cells activates VEGFR2 and an invasive phenotype: prevention by novel synstatins. *Oncogenesis* **5**, e202. doi:10.1038/oncsis.2016.5

Katada, T. (2012). The inhibitory G protein G(i) identified as pertussis toxin-catalyzed ADP-ribosylation. *Biol. Pharm. Bull.* **35**, 2103-2111. doi:10.1248/bpb.b212024

Katritch, V., Cherezov, V. and Stevens, R. C. (2013). Structure-function of the G protein-coupled receptor superfamily. *Annu. Rev. Pharmacol. Toxicol.* **53**, 531-556. doi:10.1146/annurev-pharmtox-032112-135923

Kaur, S., Chang, T., Singh, S. P., Lim, L., Mannan, P., Garfield, S. H., Pendrak, M. L., Soto-Pantoja, D. R., Rosenberg, A. Z., Jin, S. et al. (2014). CD47 signaling regulates the immunosuppressive activity of VEGF in T cells. *J. Immunol.* **193**, 3914-3924. doi:10.4049/jimmunol.1303116

Kelly, T., Miao, H. Q., Yang, Y., Navarro, E., Kussie, P., Huang, Y., MacLeod, V., Casciano, J., Joseph, L., Zhan, F. et al. (2003). High heparanase activity in multiple myeloma is associated with elevated microvessel density. *Cancer Res.* **63**, 8749-8756.

Kim, J., Mori, T., Chen, S. L., Amersi, F. F., Martinez, S. R., Kuo, C., Turner, R. R., Ye, X., Bilchik, A. J., Morton, D. L. et al. (2006). Chemokine receptor CXCR4 expression in patients with melanoma and colorectal cancer liver metastases and the association with disease outcome. *Ann. Surg.* **244**, 113-120. doi:10.1097/01.sla.0000217690.65909.9c

Kopparapu, P. K., Boorjian, S. A., Robinson, B. D., Downes, M., Gudas, L. J., Mongan, N. P. and Persson, J. L. (2013). Expression of VEGF and its receptors VEGFR1/VEGFR2 is associated with invasiveness of bladder cancer. *Anticancer Res.* **33**, 2381-2390.

Mailankody, S., Devlin, S. M., Korde, N., Lendvai, N., Lesokhin, A., Landau, H., Hassoun, H., Ballagi, A., Ekman, D., Chung, D. J. et al. (2017). Proteomic profiling in plasma cell disorders: a feasibility study. *Leuk. Lymphoma* **58**, 1757-1759. doi:10.1080/10428194.2016.1258699

Maisnar, V., Touskova, M., Tichy, M., Krejsek, J., Chrobak, L., Voglova, J. and Maly, J. (2006). The significance of soluble CD138 in diagnosis of monoclonal gammopathies. *Neoplasma* **53**, 26-29.

Massia, S. P. and Hubbell, J. A. (1992). Vascular endothelial cell adhesion and spreading promoted by the peptide REDV of the IIICS region of plasma fibronectin is mediated by integrin α4β1. *J. Biol. Chem.* **267**, 14019-14026.

May, A. E., Neumann, F. J., Schomig, A. and Preissner, K. T. (2000). VLA-4 (α4β1) engagement defines a novel activation pathway for β2 integrin-dependent leukocyte adhesion involving the urokinase receptor. *Blood* **96**, 506-513.

Molhoek, K. R., Erdag, G., Rasamny, J. K., Murphy, C., Deacon, D., Patterson, J. W., Slingluff, C. L., Jr. and Brautigan, D. L. (2011). VEGFR-2 expression in human melanoma: revised assessment. *Int. J. Cancer* **129**, 2807-2815. doi:10.1002/ijc.25963

Mullen, J. T., Vartanian, T. K. and Atkins, M. B. (2008). Melanoma complicating treatment with natalizumab for multiple sclerosis. *N. Engl. J. Med.* **358**, 647-648. doi:10.1056/NEJMc0706103

Ngo, H. T., Leleu, X., Lee, J., Jia, X., Melhem, M., Runnels, J., Moreau, A.-S., Burwick, N., Azab, A. K., Roccaro, A. et al. (2008). SDF-1/CXCR4 and VLA-4 interaction regulates homing in Waldenstrom macroglobulinemia. *Blood* **112**, 150-158. doi:10.1182/blood-2007-12-129395

Nishiya, N., Kiosses, W. B., Han, J. and Ginsberg, M. H. (2005). An α4 integrin-paxillin-Arf-GAP complex restricts Rac activation to the leading edge of migrating cells. *Nat. Cell Biol.* **7**, 343-352. doi:10.1038/ncb1234

Nóbrega-Pereira, S., Caiado, F., Carvalho, T., Matias, I., Graca, G., Goncalves, L. G., Silva-Santos, B., Norell, H. and Dias, S. (2018). VEGFR2-mediated reprogramming of mitochondrial metabolism regulates the sensitivity of acute myeloid leukemia to chemotherapy. *Cancer Res.* **78**, 731-741. doi:10.1158/0008-5472.CAN-17-1166

Oldham, W. M. and Hamm, H. E. (2006). Structural basis of function in heterotrimeric G proteins. *Q. Rev. Biophys.* **39**, 117-166. doi:10.1017/S0033583506004306

Orecchia, P., Conte, R., Balza, E., Petretto, A., Mauri, P., Mingari, M. C. and Carnemolla, B. (2013). A novel human anti-syndecan-1 antibody inhibits vascular maturation and tumour growth in melanoma. *Eur. J. Cancer* **49**, 2022-2033. doi:10.1016/j.ejca.2012.12.019

Peled, A., Kollet, O., Ponomaryov, T., Petit, I., Franitza, S., Grabovsky, V., Slav, M. M., Nagler, A., Lider, O., Alon, R. et al. (2000). The chemokine SDF-1 activates the integrins LFA-1, VLA-4, and VLA-5 on immature human $CD34^+$ cells: role in transendothelial/stromal migration and engraftment of NOD/SCID mice. *Blood* **95**, 3289-3296. doi:10.1634/stemcells.20-3-259

Purushothaman, A., Uyama, T., Kobayashi, F., Yamada, S., Sugahara, K., Rapraeger, A. C. and Sanderson, R. D. (2010). Heparanase-enhanced shedding of syndecan-1 by myeloma cells promotes endothelial invasion and angiogenesis. *Blood* **115**, 2449-2457. doi:10.1182/blood-2009-07-234757

Rasmussen, S. G. F., DeVree, B. T., Zou, Y., Kruse, A. C., Chung, K. Y., Kobilka, T. S., Thian, F. S., Chae, P. S., Pardon, E., Calinski, D. et al. (2011). Crystal structure of the β2 adrenergic receptor-Gs protein complex. *Nature* **477**, 549-555. doi:10.1038/nature10361

Rose, D. M., Cardarelli, P. M., Cobb, R. R. and Ginsberg, M. H. (2000). Soluble VCAM-1 binding to α4 integrins is cell-type specific and activation dependent and is disrupted during apoptosis in T cells. *Blood* **95**, 602-609. doi:10.1182/blood.v95.2.602

Rose, D. M., Grabovsky, V., Alon, R. and Ginsberg, M. H. (2001). The affinity of integrin α4β1 governs lymphocyte migration. *J. Immunol.* **167**, 2824-2830. doi:10.4049/jimmunol.167.5.2824

Rose, D. M., Liu, S., Woodside, D. G., Han, J., Schlaepfer, D. D. and Ginsberg, M. H. (2003). Paxillin binding to the α4 integrin subunit stimulates LFA-1 (integrin αLβ2)-dependent T cell migration by augmenting the activation of focal adhesion kinase/proline-rich tyrosine kinase-2. *J. Immunol.* **170**, 5912-5918. doi:10.4049/jimmunol.170.12.5912

Rovati, G. E., Capra, V. and Neubig, R. R. (2007). The highly conserved DRY motif of class A G protein-coupled receptors: beyond the ground state. *Mol. Pharmacol.* **71**, 959-964. doi:10.1124/mol.106.029470

Salon, J. A., Lodowski, D. T. and Palczewski, K. (2011). The significance of G protein-coupled receptor crystallography for drug discovery. *Pharmacol. Rev.* **63**, 901-937. doi:10.1124/pr.110.003350

Sanz-Rodriguez, F., Hidalgo, A. and Teixido, J. (2001). Chemokine stromal cell-derived factor-1α modulates VLA-4 integrin-mediated multiple myeloma cell adhesion to CS-1/fibronectin and VCAM-1. *Blood* **97**, 346-351. doi:10.1182/blood.V97.2.346

Scala, S., Ottaiano, A., Ascierto, P. A., Cavalli, M., Simeone, E., Giuliano, P., Napolitano, M., Franco, R., Botti, G. and Castello, G. (2005). Expression of CXCR4 predicts poor prognosis in patients with malignant melanoma. *Clin. Cancer Res.* **11**, 1835-1841. doi:10.1158/1078-0432.CCR-04-1887

Schlesinger, M. and Bendas, G. (2015). Contribution of very late antigen-4 (VLA-4) integrin to cancer progression and metastasis. *Cancer Metastasis Rev.* **34**, 575-591. doi:10.1007/s10555-014-9545-x

Smrcka, A. V. (2008). G protein βγ subunits: central mediators of G protein-coupled receptor signaling. *Cell. Mol. Life Sci.* **65**, 2191-2214. doi:10.1007/s00018-008-8006-5

Soodgupta, D., Zhou, H., Beaino, W., Lu, L., Rettig, M., Snee, M., Skeath, J., DiPersio, J. F., Akers, W. J., Laforest, R. et al. (2016). Ex vivo and in vivo evaluation of overexpressed VLA-4 in multiple myeloma using LLP2A imaging agents. *J. Nucl. Med.* **57**, 640-645. doi:10.2967/jnumed.115.164624

Stopeck, A. T., Unger, J. M., Rimsza, L. M., Bellamy, W. T., Iannone, M., Persky, D. O., Leblanc, M., Fisher, R. I. and Miller, T. P. (2009). A phase II trial of single agent bevacizumab in patients with relapsed, aggressive non-Hodgkin lymphoma: southwest oncology group study S0108. *Leuk. Lymphoma* **50**, 728-735. doi:10.1080/10428190902856808

Sunahara, R. K. and Taussig, R. (2002). Isoforms of mammalian adenylyl cyclase: multiplicities of signaling. *Mol. Interv.* **2**, 168-184. doi:10.1124/mi.2.3.168

Tada, Y., Togashi, Y., Kotani, D., Kuwata, T., Sato, E., Kawazoe, A., Doi, T., Wada, H., Nishikawa, H. and Shitara, K. (2018). Targeting VEGFR2 with Ramucirumab strongly impacts effector/activated regulatory T cells and $CD8^+$ T cells in the tumor microenvironment. *J. Immunother. Cancer* **6**, 106. doi:10.1186/s40425-018-0403-1

Taichman, D. B., Cybulsky, M. I., Djaffar, I., Longenecker, B. M., Teixidó, J., Rice, G. E., Aruffo, A. and Bevilacqua, M. P. (1991). Tumor cell surface α4β1 integrin mediates adhesion to vascular endothelium: demonstration of an interaction with the N-terminal domains of INCAM-110/VCAM-1. *Cell Regul.* **2**, 347-355. doi:10.1091/mbc.2.5.347

Teicher, B. A. and Fricker, S. P. (2010). CXCL12 (SDF-1)/CXCR4 pathway in cancer. *Clin. Cancer Res.* **16**, 2927-2931. doi:10.1158/1078-0432.CCR-09-2329

Vornicova, O., Boyango, I., Feld, S., Naroditsky, I., Kazarin, O., Zohar, Y., Tiram, Y., Ilan, N., Ben-Izhak, O., Vlodavsky, I. et al. (2016). The prognostic significance of heparanase expression in metastatic melanoma. *Oncotarget* **7**, 74678-74685. doi:10.18632/oncotarget.12492

Walenkamp, A. M. E., Lapa, C., Herrmann, K. and Wester, H.-J. (2017). CXCR4 ligands: the next big hit? *J. Nucl. Med.* **58**, 77S-82S. doi:10.2967/jnumed.116.186874

Wang, H., Jin, H. and Rapraeger, A. C. (2015). Syndecan-1 and Syndecan-4 capture epidermal growth factor receptor family members and the α3β1 integrin via binding sites in their ectodomains: novel synstatins prevent kinase capture and inhibit α6β4-integrin-dependent epithelial cell motility. *J. Biol. Chem.* **290**, 26103-26113. doi:10.1074/jbc.M115.679084

Wescott, M. P., Kufareva, I., Paes, C., Goodman, J. R., Thaker, Y., Puffer, B. A., Berdougo, E., Rucker, J. B., Handel, T. M. and Doranz, B. J. (2016). Signal transmission through the CXC chemokine receptor 4 (CXCR4) transmembrane helices. *Proc. Natl. Acad. Sci. USA* **113**, 9928-9933. doi:10.1073/pnas.1601278113

Wheeler, K. C., Jena, M. K., Pradhan, B. S., Nayak, N., Das, S., Hsu, C. D., Wheeler, D. S., Chen, K. and Nayak, N. R. (2018). VEGF may contribute to macrophage recruitment and M2 polarization in the decidua. *PLoS ONE* **13**, e0191040. doi:10.1371/journal.pone.0191040

Wu, B., Chien, E. Y. T., Mol, C. D., Fenalti, G., Liu, W., Katritch, V., Abagyan, R., Brooun, A., Wells, P., Bi, F. C. et al. (2010). Structures of the CXCR4 chemokine GPCR with small-molecule and cyclic peptide antagonists. *Science* **330**, 1066-1071. doi:10.1126/science.1194396

Wu, X., Yu, T., Bullard, D. C. and Kucik, D. F. (2012). SDF-1α (CXCL12) regulation of lateral mobility contributes to activation of LFA-1 adhesion. *Am. J. Physiol. Cell Physiol.* **303**, C666-C672. doi:10.1152/ajpcell.00190.2012

Yang, Y., MacLeod, V., Miao, H.-Q., Theus, A., Zhan, F., Shaughnessy, J. D., Jr., Sawyer, J., Li, J.-P., Zcharia, E., Vlodavsky, I. et al. (2007). Heparanase enhances syndecan-1 shedding: a novel mechanism for stimulation of tumor growth and metastasis. *J. Biol. Chem.* **282**, 13326-13333. doi:10.1074/jbc.M611259200

Zhu, P., Hu, C., Hui, K. and Jiang, X. (2017). The role and significance of $VEGFR2^+$ regulatory T cells in tumor immunity. *Onco. Targets Ther.* **10**, 4315-4319. doi:10.2147/OTT.S142085

Ziogas, A. C., Gavalas, N. G., Tsiatas, M., Tsitsilonis, O., Politi, E., Terpos, E., Rodolakis, A., Vlahos, G., Thomakos, N., Haidopoulos, D. et al. (2012). VEGF directly suppresses activation of T cells from ovarian cancer patients and healthy individuals via VEGF receptor Type 2. *Int. J. Cancer* **130**, 857-864. doi:10.1002/ijc.26094